GEOWISSENSCHAFTLICHE MITTEILUNGEN

Heft 14

Self Checking Analytical Relative Orientation and Strip Formation

von

L. MOLNAR

GEOWISSENSCHAFTLICHE MITTEILUNGEN

Heft 14

Self Checking Analytical Relative Orientation and Strip Formation

von
L. MOLNAR

SUMMARY

A new mathematical procedure is suggested for relative orientation of
aerial photographs. The procedure is theoretically interesting, provides
a simple geometric meaning of residuals, it is effective in execution,
and suits advantageously the subsequent processes of model connection
and strip homogenization.

A process of strip homogenization is proposed to be solved simultaneously
for each strip following the relative orientation of photographs and
preliminary model connection. The process is mathematically simple, and
provides advantages similar to those of a triplet triangulation.

The concept of "geometric weights" is introduced into the theory of
adjustment computations. This concept facilitates greatly the geometric
understanding of adjustments. It is very important in network planning,
and in processes of blunder detection.

With the help of the geometric weight concept, the interrelation of
different technics of blunder detection is treated (Baarda, Kraus, Stefanovic).
In this, relationships of eminent theoretical and practical importance have
been introduced.

The results of theoretical investigations are realized in the system
of two programs PHOTO and MODEL. These programs are the most current
stage in a process of 14 years of research, program development, and
of production application.

Contents

INTRODUCTION

Programs for relative orientation and model connection (strip formation)
are basic pieces of application software in analytical photogrammetry.
They should be systematically updated. This is not always done because
present day computational costs are low while the creation of new
software is expensive. The result is a tendency toward technical
conservatism which is manifested in the use of far outdated programs
by many photogrammetric organizations.

Requirements for more universal programs follow from the application of
the same aerial triangulation software for diverse purposes in diverse
areas spread over continents. This occurs by international firms or in
the case of software purchase.

Blunder detection is one of the main tasks of applying differentiated pro-
cesses of analytical aerial triangulation as a preparatory stage to a
final simultaneous adjustment. This is important in both technical and
economical respects. The task of preliminary blunder detection and
elimination in the processes of relative orientation and strip formation
can now be solved satisfactorily by applying the newest developments in
least squares techniques, and by refining the differentiated analytical
processes themselves, so to be able to cope with "small blunders"
effectively.

At the same time, refined differentiated processes yield better preliminary
coordinates for the following simultaneous adjustment. When applying a
block adjustment of "independent models" following these refined
analytical processes, one can replace strip sections for single models.
As practice indicates, no noticeable accuracy decrease occurs when using
sections of two models, and accuracy decreases just slightly when using
sections of three models. Adjustment of sections rather than single
models can be performed with computation times drastically decreased /20/.

There is an increasing interest in analytical plotters these years. A
wider spread of this technique in photogrammetric production will mean
strong demand in improved software.

All these points make the old, out of fashion subject of analytical
relative orientation and strip formation a current issue. Considering
it is divided in this work into two interrelated parts. The first one

with theoretical and practical questions of mainly photogrammetrical character, and the second one belonging more to the realm of adjustment computations and featuring questions of blunder detection and elimination.

The theoretical and practical points treated in this report are realized in a system of the two programs PHOTO and MODEL. These programs are the most current stage in a long process of research, program development, and of production application (3 independent ALGOL versions in Hungary, 1965-72; completely new FORTRAN programs in the U.S., in two versions, 1975-77; and the current, completely re-written and nearly doubled in size FORTRAN programs running on the CDC Cyber 74 of the Technical University of Vienna, Austria). PHOTO and MODEL match the requirements of mass production in analytical aerial triangulation.

1. PHOTOGRAMMETRIC ASPECTS

1.1 General description of the major processes in the programs [+)]

1.1.1 Data registered on stereo or monocomparators are preprocessed by program PHOTO. The aims of the processes involved are:

- formal checking,
- determining image coordinates corrected for systematic influences (film deformation, refraction, and optical distorsion),
- preliminary checking of data sufficiency.

Notes on and formulas of taking into account systematic image coordinate errors are given in Appendix I. Appendix II. contains an example of a REPORT file.

Photographs may be read in any arbitrary position (positive or negative, emulsion up or down, arbitrary kappa-orientation). All these cases are universally converted into some common case determined by the elements of interior orientation of the camera (focal length, x and y displacements of the projection center, calibrated fiducial coordinates and distortion

---

[+)] Although the FORTRAN text of the programs is now more than 3500 cards long, their structure is suitable for overlaying. Therefore they can be adjusted to computers as small as a DEC PDP 11-34.

coefficients). The choice of the coordinate system for interior orientation influences the sign of the elements of relative orientation and of model (strip) coordinates yielded by the procedure.

Working with stereocomparators, the photograph read in right side position for one model is read again in left side position for the next model. These readings are combined by taking the fiducial readings in the right side position as basis, and transforming the readings in the left side position by the formulas applied later on for fiducial transformation. This process of "left-to-right position transformation" offers a safe way of blunder detection in fiducial readings. The combined readings are then transformed applying the calibrated coordinates of fiducials or some replacement for them. Statistics of these "fiducial transformations" yield characteristics of film deformation of photographs within each strip.

1.1.2 Program MODEL performs the following major processes:

- relative orientation of photographs,
- model connection (strip formation),
- post-processing of each strip to refine homogeneity,
- printing tables of statistics.

Details on these processes are to be found in the next chapters.

1.2   Relative orientation of photographs

1.2.1 Review

From a purely mathematical point of view it is certainly impossible to show decisive advantages of one properly applied way of relative orientation over another. There are, however, other respects influencing a choice. In this sense the following advantages are inherent to the method described below:

- photogrammetric obviousness of the geometry and of residuals,
- easy of strip formation,
- geometry consistent with the post-processing stage,
- simplicity and effectivness of the linearized correction equation.

Changing the spatial position of the right projection center is the main geometric peculiarity of this method. In this way a new right side photograph is constructed which forms a normal stereogram with the left photograph. The position of the preceding (left side) photograph is not changed within the process of relative orientation (this last moment being common with the widely spread method of Shut /1/).

Such geometry of relative orientation has a rich past in the Russian photogrammetry. Thechnologies presupposing the presence of a highly developed optical industry were not acceptable to Russian photogrammetrists in the early 1930-s. The solution is due to Drobishew who constructed the famous stereometer. Stereometers are portable photogrammetric instruments, theoretically based upon analytical relative orientation and solving the corresponding equations for x-coordinates by correction mechanisms. The mechanisms have to be set to the elements of relative orientation. And this is the point: such elements were determined by computation, based upon stereocomparator measurements. The corresponding simplified theory and procedure were created by Zhukow. This solution resulted in a mass production in analytical photogrammetry as early as the middle 1930-s /2/. Numerous refinements of the Zhukow procedure have been published later in the Russian photogrammetric literature.

Unlike these methods the relative orientation procedure described here is thought to be applied in modern computer programs, and therefore it does not contain any neglections.

As to a classification of methods of relative orientation one could suggest to differentiate between those methods determining the spatial position and orientation of the original bundles of rays (class 1), and those constructing normal stereograms (class 2). In both cases it is possible to fix the origin and orientation of the model coordinate system to the base, as done by Lobanoff for the first class of methods /5/, and by Urmajew for the second /10/; or to fix the origin and orientation of the model coordinate system to the left photograph, as done, for the first class of methods, by Shut /1/ and Jerie /3/, and by the method described in this work for the second class. This last case involves the computational creation of a third bundle of rays.

1.2.2 Deduction of equations for relative orientation

The derivation of needed formulas is divided here into two major steps, both of which are common and simple. The first step takes care of the angular elements of relative orientation ω, ϕ and κ, all of them related to the right side photograph. Having performed the corresponding transformation, we arrive at the situation shown in Fig. 1 by the photograph with projection center at S" whose axes $x_t''y_t''z_t''$ are parallel to those of the left photograph. The second step considers then the base elements B_y and B_z.

1.2.2.1 Rotational elements of the right side photograph

In order not to lose the geometric image which photogrammetrists are accustomed to, a trigonometric solution is applied. In particular, one in which the rotation around the Y axis (ϕ) is considered as secondary. The corresponding formulas:

$$X_t'' = A x'' \tag{1.1}$$

where

$$X_t'' = \begin{bmatrix} X_t'' \\ Y_t'' \\ Z_t'' \end{bmatrix} \qquad \text{with } Z_t'' \neq -c$$

$$X'' = \begin{bmatrix} X'' \\ Y'' \\ Z'' \end{bmatrix} \qquad \text{with } z'' = -c$$

$$A = \begin{bmatrix} a_{11} & a_{12} & a_{13} \\ a_{21} & a_{22} & a_{23} \\ a_{31} & a_{32} & a_{33} \end{bmatrix}$$

$a_{11} = \cos\phi \cos\kappa$ $\qquad a_{13} = \sin\phi$

$a_{21} = \cos\omega \sin\kappa + \sin\omega \sin\phi \cos\kappa$ $\qquad a_{23} = -\sin\omega \cos\phi$

$a_{31} = \sin\omega \sin\kappa - \cos\omega \sin\phi \cos\kappa$ $\qquad a_{33} = \cos\omega \cos\phi$

$a_{12} = -\cos\phi \sin\kappa$

$a_{22} = \cos\omega \cos\kappa - \sin\omega \sin\phi \sin\kappa$

$a_{32} = \sin\omega \cos\kappa + \cos\omega \sin\phi \sin\kappa$

(1.1) expresses a mathematical transformation. In photogrammetry the word transformation means more than that. We must determine the intersection of the rotated (by the mathematical transformation) bundle of rays with the plane of the new photograph to be constructed. This is solved by the formula

$$x''_t = - \frac{c}{z''_t} X''_t \quad \text{where} \quad x''_t = \begin{bmatrix} x''_t \\ y''_t \\ z''_t \end{bmatrix} \quad \text{with} \quad z''_t = -c \qquad (1.2)$$
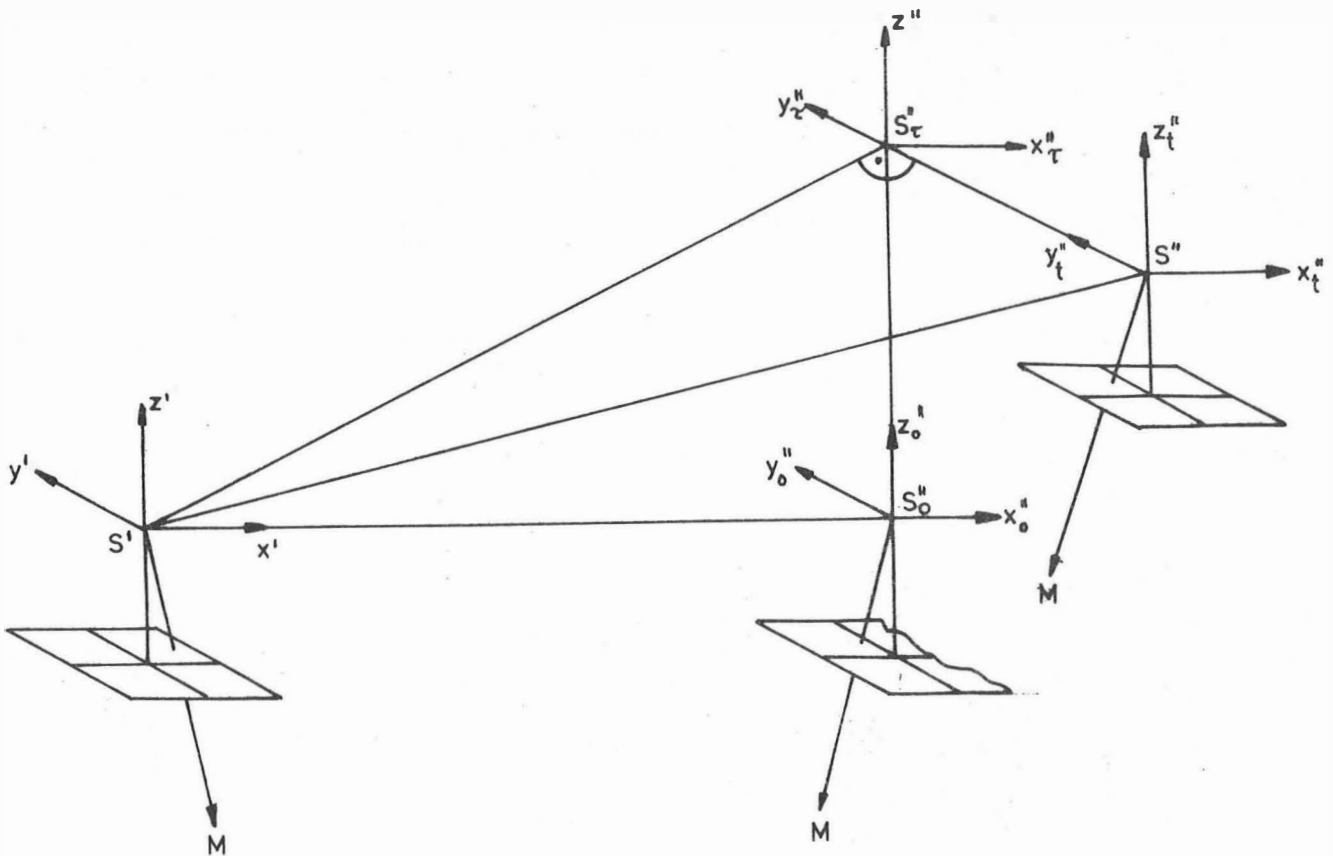
Fig.1: S' is the projection center of the left photograph. The axes of the photo coordinate system of it (x'y'z') are taken as coordinate system of the model to be created. The right side photograph with projection center S" has been transformed into a position parallel to the xy-plane of the left photograph. (Axes x''_t y''_t z''_t are parallel to x' y' z'). S"_o is the projection center of the new right side photograph to be created analytically in the process of relative orientation. The plane S"S"_τ S"_O is perpendicular to the plane S'S"_τ S"_O, and S"_τ is the orthogonal projection of S" onto this last plane. M is an arbitrary point of the terrain.

1.2.2.2 Projection center movements (base elements)

The expressions which take care of the projection center movements or, in other words, of the base elements, can be derived using Fig. 1.

In final expressions, instead of speaking in terms of the linear movements of B_y and B_z, we use correspondingly, ν and τ. In exact terms,

$$\tan \tau = \frac{B_z}{B_x} \qquad (1.3)$$

and

$$\tan \nu = \frac{B_y}{B_x} \qquad (1.4)$$

Expressions have to be derived expressing y''_o and x''_o of the right photograph of the normal stereogram. It is important to note that this is a new photograph to be numerically constructed, as opposed to a changed position of the original right photograph attained by transformation. This point will become obvious later.

1.2.2.2.1 Expression for $y''_o = f(x',y',x''_t,y''_t,\tau,\nu)$

The determinants written below are equal to 0 because of the coplanarity of the participating vectors: of some base vector $\overline{S'S''}$ connecting two projection centers, and of two other vectors pointing from these projection centers to the corresponding images of the terrain point M. To shorten the description such cases will be referred to just by (S'S''M), always applying the corresponding projection centers. Notations correspond to fig.1. The index t refers to photographs transformed by ω, ϕ and κ.

(S'S''M):

$$\begin{vmatrix} B_x & B_y & B_z \\ x' & y' & -c \\ x''_t & y''_t & -c \end{vmatrix} = 0$$

Taking into consideration (1.3) and (1.4), and rearranging the expression:

$$\frac{x'y''_t - x''_t y'}{c} \tan\tau + (x'-x''_t)\tan \nu - (y'-y''_t) = 0 \qquad (1.5)$$

$(S'S''_oM)$:

$$\begin{vmatrix} Bx & 0 & 0 \\ x' & y' & -c \\ x''_o & y''_o & -c \end{vmatrix} = 0$$

This determinant is the <u>photogrammetric</u> co-planarity condition in our case of relative orientation, and expresses the equality of corresponding y photo coordinates in normal stereograms:

$$y' = y''_o \tag{1.6}$$

(1.5) and (1.6) yield the sought expression for y''_o :

$$y''_o = y''_t + \frac{x'y''_t - x''_t y'}{c} \tan\tau + (x' - x''_t)\tan\nu \tag{1.7}$$

Because of errors of different origin, summarized as observation errors, remainder vertical parallaxes are always present, and therefore (1.6) has to be rewritten as

$$y' - y''_o = p_{yo} = -v \tag{1.8}$$

where $p_{yo} \simeq 0$ is the vertical parallax in the constructed normal stereogram, or, in other words, the remainder vertical parallax. Comparing expressions (1.5) to (1.8) the corresponding observation equation can be written:

$$\frac{x'y''_t - x''_t y'}{f} \tan\tau + (x' - x''_t)\tan\nu - (y' - y''_t) = v \tag{1.9}$$

As $\tan\tau$ and $\tan\nu$ are taken directly as unknowns in this process, (1.9) is linear (with regard to $\tan\tau$ and $\tan\nu$).

1.2.2.2.2 <u>Expression for $x''_o = f(x', y', x''_t, y''_t, \tau, \nu)$</u>

The expression for x''_o plays an important role in computing model coordinates. This way it conveys the inaccuracy of relative orientation to these coordinates. Therefore care should be taken in deriving the expression for x''_o: some ways of derivation yield formulas which may enlarge the influence of the inaccuracies mentioned.

$(S_\tau'' S_0'' M)$:

$$
\begin{vmatrix}
0 & 0 & B_z \\
x_\tau'' & y_\tau'' & -c \\
x_0'' & y_0'' & -c
\end{vmatrix} = 0
$$

which yields

$$
x_0'' = \frac{y_0''}{y_\tau''}\, x_\tau'' \tag{1.10}
$$

$(S'' S_\tau'' M)$:

$$
\begin{vmatrix}
0 & B_y & 0 \\
x_t'' & y_t'' & -c \\
x_\tau'' & y_\tau'' & -c
\end{vmatrix} = 0
$$

and therefore

$$
x_\tau'' = x_t'' \tag{1.11}
$$

(1.11) expresses the fact known from terrestrial photogrammetry that B_y (B_z in terrestrial notation) does not influence the x coordinates. This is why height differences of camera stations can be neglected in the "normal" case of terrestrial photogrammetry.

$(S' S_\tau'' M)$:

$$
\begin{vmatrix}
B_x & 0 & B_z \\
x' & y' & -c \\
x_\tau'' & y_\tau'' & -c
\end{vmatrix} = 0
$$

which yields, after some elementary steps:

$$
y_\tau'' = \frac{c + x_t''\, \tan\tau}{c + x'\, \tan\tau}\, y' \tag{1.12}
$$

(1.10) to (1.12) combined:

$$x_o'' = x_t'' \frac{y_o''}{y'} \quad \frac{c + x' \tan\tau}{c + x_t'' \tan\tau} \tag{1.13}$$

The number of this formula, 13, indicates probably the danger connected with it: the factor y_o''/y' must be taken for 1. This may be done if no rude errors are present. Blunder detection and elimination are solved satisfactorily (part 2 $^)$, and therefore (1.13) can be replaced by

$$x_o'' = x_t'' \frac{c + x' \tan\tau}{c + x_t'' \tan\tau} \tag{1.14}$$

Another way of deduction yields the following unsatisfactory expression for x_o'' :

$$x_o'' = x_t'' \frac{y' - x' \tan\nu}{y_t'' - x_t'' \tan\nu}.$$

A still further dangerous expression is:

$$x_o'' = x_t'' \frac{c \tan\nu - y_o'' \tan\tau}{c \tan\nu - y_t'' \tan\tau}$$

1.2.2.2.3 The geometric meaning of the recursivity

Formulas (1.7), (1.9), and (1.14) are recursive because of using x_t'' and y_t'' on the "right side". These values become precise only in the final iteration steps.

This recursivity cannot be eliminated and it has a very certain photogrammetric meaning: a photograph "taken" from an arbitrary "third" point can only be constructed if the model of the terrain has already been reconstructed. In other words, the change of the spatial position of a projection center is a stereophotogrammetric task. Were this not so, we could construct a second photograph of the terrain using just one photo, and then count the terrain heights using the old and the constructed photographs as a pair.

One solves recursive expressions by iterations. The same is needed by using least squares techniques for non-linear equations anyway. Therefore, the above recursivity does not mean further complication to the process in this respect.

1.2.2.3 The iterative process

The process of iterations takes into consideration the geometric fact that transforming a single photograph by expression (1.2), using any arbitrary values for ω, ϕ and κ is a rigorous process. This means that the erroneousness of the elements will not distort the corresponding bundle of rays. Using the not quite precise elements $\delta\omega, \delta\phi$, and $\delta\kappa$ of the last iteration, applying expressions (1.2) to the right side photograph, one gets a geometrically new situation which can be handled as if no iterations had been completed before. The final values for ω, ϕ and κ will mean, in this case, the sum of the values $\delta\omega$, $\delta\phi$ and $\delta\kappa$ gained in the course of consecutive iterations.

Because of the geometrical circumstance in connection with the recursivity of expression (1.9) we cannot apply the same approach to the base elements τ and ν . The coefficients of (1.9) are updated after each iteration. Using these updated observation equations the entire values of $\tan\tau$ and $\tan\nu$ are determined again and again.

Taking the above into consideration, the linearization of (1.9) can be reduced to the linearization of the corresponding row in (1.2). (1.2) and (1.9) yield:

$$(c+\frac{y_t''^2}{c})\delta\omega- \frac{x_t'' \, y_t''}{c} \delta\phi +x_t''\delta\kappa + \frac{x'y_t''-x_t''y'}{c} \tan\tau +(x'-x_t'')\tan\nu -(y'-y_t'') = v$$

$$(1.21)$$

where x_t'', y_t'' are coordinates of the right side photo, transformed by
        (1.2) due to ω, ϕ, and κ of the (n-1) th iteration; in the
        0-th iteration ω , ϕ, and κ of the previous model will be
        used, or - as an option of program MODEL - given first
        approximations;

        $\omega = \Sigma\delta\omega$ $\phi = \Sigma\delta\phi$ $\kappa = \Sigma\delta\kappa$
      $\tau = \arctan(\tan\tau)$, and $\nu = \arctan(\tan\nu)$

(1.21) appears as if it would not contain any non-linear terms. This is partly due to the updating of x_t'' and y_t'' coordinates in each iteration, which makes the process rigorous in the sence of Pope's notes /4/; and partly due to the use of $(\tan \tau)$ and $(\tan \nu)$ directly as unknowns.

The described mathematical model needs a relatively small amount of computations for each iteration, and the convergence of the process is no worse or better than that of the widely applied relative orientation procedures /1,5/.

1.2.2.4 A second system of formulas

It is interesting in some theoretical, pedagogical and historical respects that the formulas derived in this chapter 1.2.2 can be transverted into expressions written as functions of just photo coordinates of the normal stereogram to be constructed. The expressions gained can be useful when applied, for instance, in mechanical analogue constructions similar to Stereometers mentioned earlier.

The corresponding derivations are given in Appendix IV, and yield a second system of formulas.

1.2.2.5 Computing model coordinates

Having performed the relative orientation in the described way, one can use very simple formulas for computing the model coordinates - because a normal stereogram has been constructed:

$$X_{mod} = \frac{B_x}{P_{xo}} \ x \qquad (1.22)$$

where

$$X_{mod} = \begin{bmatrix} X_{mod} \\ Y_{mod} \\ Z_{mod} \end{bmatrix} \qquad \text{and} \quad x = \begin{bmatrix} x' \\ \dfrac{y'+y_o''}{2} \\ -c \end{bmatrix}$$

and

$$P_{xo} = x'-x_o''$$

In program MODEL B_x is taken equal to the mean value of p_x of the first model of the strip. This results in model coordinates approximately in photo scale. The mean value of p_x is equal to some .90 mm-s in the very typical case of a 23x23 cm^2 format and 60 % overlapping. If this value is between 80 an 100 mm-s, B_x of the first model of a strip is taken to be equal to 100 mm-s. This is advantageous in finding points on the basis of their X strip coordinates (an X strip coordinate equal, for instance, to 550 mm, will mean roughly that the corresponding point is to be found in the area of the 6-th model).

1.2.2.5 Strip formation by scaling and shifting the model coordinate systems

The x, y and z axes of the first photograph of the strip are accepted as X, Y and Z axes of the strip. The model coordinate system of the first model is automatically this system. The angular elements of relative orientation of the first two photos ω, ϕ and κ determine the orientation of the second photograph in the coordinate system of the strip. Therefore, transforming the second photograph - using expressions (1.2) - by these elements the plane of this photo becomes parallel to the XY plane of the strip system. The reader will understand at this point that it is possible to perform the transformation of the second photo by (1.2) but the task of moving the second projection center to a new position, shifting it by B_y and B_z of the previous model, is not solvable for the part of this photo which belongs to the second model: the second model has not yet been reconstructed. Performing a relative orientation by the described method after this transformation, the model coordinate system of the second model will be parallel to the strip coordinate system - but its origin displaced by B_x, B_y and B_z of the first model. One could count and use these values to shift the two systems together, but instead gravity center coordinates of passpoints have been applied for this purpose, more advantageous in a stochastical sense.

In general terms the described way of model connection can be represented as

$$X' = X''_0 + mIX'' \qquad (1.23.a)$$

where X' contains the strip coordinates, X''_0 the shifts of the model coordinate system (determined independently and indirectly by shifting together the gravity centers of passpoints), m denotes the scale factor,

and X" the model coordinates. In the transformation (1.23.a) the unit matrix I replaces the rotation matrix.

The scale of the model to be connected can be determined in this geometry simply as a relation of the corresponding Y' and Y" model coordinates related to the corresponding gravity centers G' and G" of passpoints. This is because, as shown below, no X model coordinate discrepancies occur, and because of the narrowness of the triple overlap zone. A normal equation with one unknown: m - the scale factor, is used for this purpose:

$$m = \frac{\left[(Y''-G''_y)(Y'-G'_y)\right]}{\left[(Y''-G''_y)^2\right]} \qquad\qquad (1.23.b)$$

1.3   Strip homogenization

One cannot overemphasize the importance of the fact that the use of two-photo   simply

_____ per _____. [+)] This is a result of basically two circumstances. First, that in such cases measurements are improperly checked (see part 2). Second, as a result of insufficient accuracy of relative orientation, model distorsions occur that are larger than generally expected. Both these interrelated problems can be essentially solved without increasing the data amount, by not neglecting the information contained in passpoints.

Triplet triangulation is the best known and most widely spread solution /8/. In this case three bundles of rays are solved each time in one system, and the "double models" gained this way joined then by spatial linear transformation.

A simple and not less adequate solution is introduced in this chapter: the homogenization of the strip gained by sequential two-photo orientations. Such postprocessing method is identical in its principle with strip homogenization in numerical analogue triangulation /11/.

The postprocessing method has to remain simple otherwise the sense of applying a differentiated way of aerial triangulation could be lost. This same is

[+)] We think it important to drow attention to this fact especially in Europe where the spread of analytical methods is just in process, and corresponding experience seems to be missing.

needed to arrive at well conditioned systems of equations. Therefore
we are considering only the linearized expressions, and thus restricting
the procedure to the "nearly vertical case" of analytical aerial
triangulation.

To gain the functions needed for strip homogenization systematic
discrepancies in model coordinates of passpoints of adjacent models have
to be analyzed as functions of errors of the relative orientation. For
this, fig. 2 will be used.
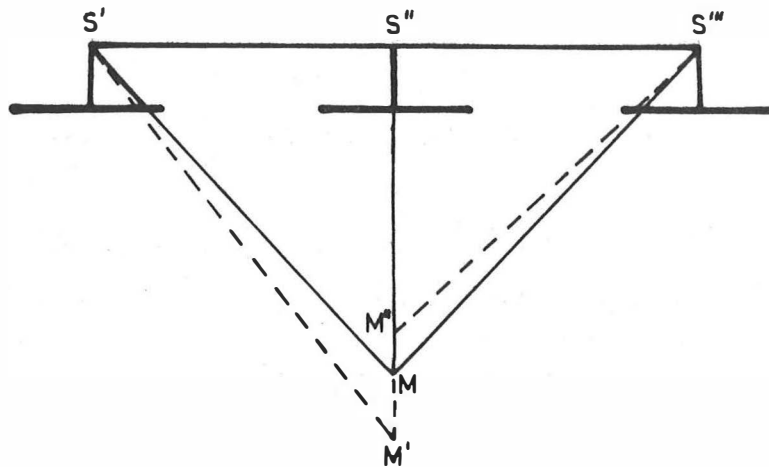
Fig. 2 *illustrating that δx', δx", or δx"' image coordinate errors
(all in x-direction) do not cause any ΔX model coordinate
discrepancies in model connection.*

Program PHOTO, when applied to stereocomparator readings, converts them
to photo coordinates as if read in a monocomparator. This way point
transfer errors distorting x" are checked and averaged (or rejected) as
reading errors in the middle photograph. As a result, no model coordinate
discrepancies occur in X. A derivation is given in Appendix V proving
the validity of this statement in a general case. Appendix III provides
the empirical proof.

Neither constant nor linear parts occur in Y-discrepancies as a result
of shifting and scaling by (1.23). The rest of Y-discrepancies, ΔY_a, is
a function of Y^2 (the derivation is given in Appendix VI). This part is
apparent as an assymmetrical error in Y:

$$\Delta Y_a = -Y^2 \left(\frac{1}{Z} \frac{\Delta\omega' + \Delta\omega''}{2} + \frac{1}{B_x} (\Delta\kappa'' - \Delta\kappa') \right) \qquad \text{(VI.4')} = \text{(1.24)}$$

with $\Delta\omega'$, $\Delta\kappa'$, $\Delta\omega''$ and $\Delta\kappa''$ indicating errors in the corresponding elements of relative orientation of two adjacent models.

Point transfer in y can be solved very precisely with point transfer devices marking, at the very least, the point on the middle photograph. Therefore (1.24) contains valuable information.

Errors of relative orientation cause very noticable discrepancies in Z that can be divided into a shift and a part which is a linear function in (Y). The shift contains the influence of errors in ϕ and τ, and disappears in the process of model connection by (1.23). The second part can be expressed, as shown in Appendix VII, as:

$$\Delta Z = YZ \left(\frac{1}{Z} (\Delta\omega' + \Delta\omega'') + \frac{1}{B} (\Delta\kappa'' - \Delta\kappa') \right) \qquad \text{(VII.2')} = \text{(1.25)}$$

(1.24) and (1.25), applied as correction equations, form the most complex way of the proposed strip homogenization.

Care schould be taken as to degrees of freedom and data distribution. Clearly, the first model has to be kept unchanged. Even though (1.24) and (1.25), when applied to a strip of just 2 models, yield a singular system. Geometrically this means that we cannot separate the influence of κ errors, resulting in a minor rotation of the model around the X-axis, from the influence of ω errors, resulting in a torsion of the model surface. - Therefore, the relative orientation of the first and last models of each strip should remain unchanged in the homogenizing process.

Good passpoint distribution yields well conditioned systems. However, if this is not the case (or there is ground for suspicion in this respect), one has to sacrifice a certain degree of flexibility, and to involve in the $v^T W v = \min$ condition the unknowns themselves (with a suitable weight, naturally). This way, undesired effects of "overcorrection" can be avoided.

In cases where only the heights have to be determined with high accuracy, the process can be considerably simplified. If the point transfer in y is not solved adequately, (1.24) has not to be applied. The surface of each model, as long as heights are concerned, becomes a hyperbolic paraboloid

as a result of errors in relative orientation /6/. We cannot correct for
the paraboloid. Therefore the homogenization can be set up with unknowns
that are parameters of the individual hyperboloids a'- b":

$$a'Y + b'XY - (a''Y + b''XY) = \Delta Z \qquad (1.26)$$

(1.26) means noneglections when compared with (1.25). A further simplifi-
cation can be considered, that of replacing hyperboloids by planes. In this
case:

$$a'Y - a''Y = \Delta Z \qquad (1.27)$$

Although (1.27) means neglections, it has a very important advantage: it
yields safe, well-conditioned systems even for relatively weak passpoint
configurations. The planes replacing the hyperboloids are symmetrically
oriented, and this way the neglection is somewhat compensated: its rest
hardly exceeds the noise level of Z-transfer errors.

Naturally, whether applying (1.26) or (1.27), the notices on degrees of
freedom and data distribution given before remain valid.

Strip homogenization with (1.27) has been applied in the practice of pro-
duction since 1975 by Berger Associates, Columbus, Ohio. Experience indi-
cates that results are, at least in Z, not only of equal quality but, as
a tendency, identical to the results of triplet triangulation /12/.

2. BLUNDER PROCESSING

As major tasks, blunder processing involves data amount and distribution checking, blunder searching (blunder detection and location), and the connected task of tolerance determination. All these can be considered on a general level, and on the level of some application - in our case that of self checking photogrammetric relative orientation and strip formation, as introduced in part 1. This second being our subject, general discussion will be kept here to a minimum with the exception of introducing the concept of geometric weights which seems to us inevitable. Otherwise three major sources of the related special literature will be cited: the pioneering work of Baarda /15/, the article of Kraus concerning practice /16/, and the recent complex study by Stefanovic /17/. Concentrating on the tasks of blunder processing in analytical relative orientation and strip formation we limit all discussions to the case of "indirect observations". Naturally, the concepts involved can be extended, without much difficulty, to other cases of least squares techniques.

2.1 Introducing the concept of geometric weight coefficient matrix

Let us consider the system of n correction equations

$$Ax = 1 + v \qquad (2.1)$$

where A is the coefficient matrix of unknowns,

x is the vector of u unknowns,

1 is the vector of observations, and

v is the vector of residuals.

r = n - u denotes the redundancy of this system, and r/n is termed as relative redundancy. When r=0 the vector of residuals v becomes 0, meaning that in such case the solution absorbes the observational errors. In an opposite extreme with all observations repeated infinite times (r=∞) no error absorption occurs, and the vector of residuals will correspond to the vector of observational errors ε. As shown in /17/, residuals and observational errors are connected by the relationship

$$v = - Q_{vv}W\varepsilon \qquad (2.2)$$

where Q_{vv} is the cofactor matrix of residuals, and $W = Q_{11}^{-1}$ is the weight matrix of observed quantities. W is an a-priori matrix and its elements do

not change in the process of adjustment. Therefore the a-posteriori matrix Q_{vv} contains the coefficients describing the error absorption in the process of adjustment.

Hungarian geodesists-practitioners apply the expression "geometric weight", and in the U.S. I have heard the expression "geometric constraint", both in the following sense: when a measured quantity has a large geometric weight it will have large influence on the unknowns to be determined, and the corresponding residual after the adjustment is expected to be small even if some rude error is distorting theat measurement. This weight or constraint is felt to be depending on data distribution and mathematical model.

Considering (2.2) it is easy to notice that <u>the error absorbing capacity</u> <u>of the process and the "geometric weights" express reciprocal tendencies.</u> <u>They are the proper interpretation of the cofactor matrix of residuals Q_{vv},</u> <u>which therefore could be given the name "geometric weight coefficient matrix".</u> This would mean, naturally, the introduction of another - a-posteriori - weight concept, being contraversial because of the danger of simplistic understanding. So the reader has to judge whether the advantages of this principle outweigh the dangers of misinterpretation.

<div align="center">*</div>

The reader will remember that the variance-covariance matrix of residuals Σ_{vv} can be written, by definition, as

$$\Sigma_{vv} = E\left[(v-\mu_v)(v-\mu_v)^T\right] = E\left[vv^T\right] - \mu_v\mu_v^T = E\left[vv^T\right]$$

with μ_v the first moment (expectation of the mean) of residuals which is equal to 0 in an unbiased adjustment, and

$$Q_{vv} = \sigma_o^{-2}\Sigma_{vv} = \sigma_o^{-2}E\left[vv^T\right] \tag{2.3}$$

where σ_o^{-2} denotes the reference variance. Appendix VIII contains a derivation of Q_{vv}.

In the case of some ideal adjustment the expectation of variance of each "homogenized" residual should be equal to the variance of the observational errors. For an adjustment free of bias the reference variance σ_o^2 is the least squares' estimate of the variance of observational errors with the a-priori weight unity. With regard to (2.3) this means that Q_{vv} should be

equal to the unit matrix I. This is the extreme case mentioned above with $r=\infty$. In the other extreme case with $r=0$ diagonal elements in Q_{vv} become 0. For all intermediate cases - where all practice belongs - these geometric weight coefficients are intermediate values, indicating the measure of error absorption in the area of each point /15/. Given this measure, residuals can be "scaled":

$$\bar{v} := \bar{Q}_{vv}^{-\frac{1}{2}} v \qquad\qquad (2.4)$$

where $\bar{Q}_{vv}$ denotes (diag Q_{vv}).

The expression "scaling of residuals" in connection with (2.4) is misleading when understood literally. Random errors in all the observations mean random tensions to the mathematical model (2.1), and therefore individual "scaled" residuals $\bar{v}_i$, being tensions introduced to the model, are in no linear relationship with observational errors. In other terms: (2.4) is not a direct consequence of (2.2). These questions will be explicitly dealt with in chapter 2.2.

<div align="center">x</div>

An often applied way of handling a-priori weights is the homogenization of the system of observational equations so to arrive at an uncorrelated equal weight situation. As a result of homogenization a-priori weights become implicit. On the other hand, "geometric weights" always have to be considered as implicitely present in the starting equations. When so understood, the "scaling of residuals" in form of (2.4) becomes natural as takint into account these weights.

The application of (2.4) yields equally accurate residuals $\bar{v}$. With them, as proven in Appendix IX, the reference variance can be counted as

$$\sigma_o^2 = \frac{1}{n} v^T \bar{Q}_{vv}^{-\frac{1}{2}} Q_{11}^{-1} \bar{Q}_{vv}^{-\frac{1}{2}} v = \frac{1}{n} \bar{v} W \bar{v} \qquad\qquad (2.5)$$

The denominator in (2.5) is the number n of observation equations because the influence of error absorption has been taken into account by (2.4). This a-posteriori homegenization is understandable with regard to (2.2), as well.

<div align="center">x</div>

It appears very obvious to interpret the role played by Q_{vv} as geometric weight coefficient matrix in <u>counting influences of partial data elimination</u> (a matter extensively treated in Stefanovic /17/).

Let us denote the residual on a point having participated in the adjustment by v^+, and the corresponding residual when the point has been removed from the adjustment by v^- (not to be mistaken for $\bar{v}$: the scaled residual in (2.4)). It is easy to comprehend the geometric meaning of processes and formulas when keeping in mind some point, loosely speaking, "of large geometric weight" and correspondingly with small diagonal geometric weight coefficient q_{ii}. E.g. in case of relative orientation of photographs some remote point standing alone in the corner of the model (2.2.3.1.1). v^+ in this point is to be expected small according to formula (2.2). The "scaled" residual $\bar{v}$ can be determined by applying (2.4) and expresses the <u>tension</u> introduced by this point into the adjustment. Removing the point from the adjustment means removing this tension. The geometric weight of the point exercises a reverse effect in this case and therefore v^- can be determined as

$$v^- = (Q^+)^{-\frac{1}{2}} \bar{v} \tag{2.6}$$

where Q^+ denotes the corresponding submatrix (the corresponding diagonal element) of Q_{vv} counted with the elements of the adjustment with the point participating. (2.6) is valid for groups of points, as well. For this, $\bar{v}$ also has to be counted with the corresponding submatrix of Q_{vv} /17/.

Submatrices of Q_{vv} include off-diagonal elements. Off-diagonal elements in Q_{vv} express the <u>functional</u> dependence of residuals. As a result of the functional dependence of residuals, Q_{vv} is singular (of rank r). In addition it is idempotent. Therefore all submatrices which are of greater size than r x r are singular. In this form the fact is expressed that the equation system cannot be solved when less than u observations are present. This means that when removing more than r points from the adjustment (2.6), looses its sense /17/.

To determine the cofactor submatrix in (2.6) as a function of elements of the new adjustment with the point(s) removed, one has to apply to (2.1) as to a function the rules of propagation of variances and covariances. The corresponding elementary deduction yields

$$Q_{ff}^- = Q_{v^-v^-} = I + A_i Q_{xx}^- A_i^T \tag{2.7}$$

where A_i is the corresponding row in the coefficient matrix of unknowns, and Q_{xx}^- is the cofactor matrix of unknowns determined in the adjustment with the point(s) removed. Comparing (2.6) and (2.7), the following equality should exist <u>when $Q_{11} = I$ (weighting is inapplicable to Q_{ff}</u>):

$$(Q^+)^{-1} = Q_{ff}^- \tag{2.8}$$

or, with more details:

$$(I - A_i Q_{xx}^+ A_i^T)^{-1} = I + A_i Q_{xx}^- A_i^T \tag{2.9}$$

This relationship, speaking for the concept of geometric weights, is proven in Appendix X.

x

Elements of Q_{vv} express the "strength of the figure" to be adjusted /15/. As Q_{vv} is counted with<u>out</u> the vector l of observed quantities, it is possible to estimate its elements in advance at the stage of <u>network planning</u>. Diagonal elements in Q_{vv} should dominate, and be close to each other in value. High mutual dependence of any two residuals has to be avoided in order to assure adequate blunder location (this involves checking the corresponding 2 x 2 submatrices of Q_{vv} on singularity). All this can be achieved by changing data amount and/or data distribution. In Baarda's words observations of a network planned this way become "equivalent": of equal unknown determining strength, and equally well checked (see later). - In this very prominent application Q_{vv} appears explicitly as "geometric weight coefficient matrix", <u>yielding numerical characteristics of the geometric quality ("strength") of the network</u>.

x

Further extremely important relationships containing Q_{vv} are given by Stefanovic /17/. All of them can be interestingly interpreted in the light of our concept. Still further examples of such interpretation will occur in the course of this work.

2.2 Blunder detection[x]

2.2.1 General

Let us exclude a point (or a group of points) from the set of data, and perform the adjustment with the rest of data. If this new set yields a well conditioned system, and contains just "random" errors (as opposed to blunders), we expect v^- of the excluded point to be equal to the observational error(s) ε:

$$E\left[v_{\overline{V}}^-\right]= \varepsilon \qquad (2.10)$$

where the index V indicates the point excluded. The accuracy of this equality can be assessed with the help of the cofactor matrices on any side of (2.8):

$$E\left[v^{-T}v^-\right]= \sigma_o^2\ Q_{ff}^- = \sigma_o^2(Q^+)^{-1} \qquad (2.11)$$

Correspondingly, in comparisons of the absolute value of v^- with some tolerance δ , this tolerance has to vary with the location of the removed point:

$$|v^-|\ \le\ \delta(Q^+)^{-\frac{1}{2}} \qquad (2.12)$$

With regard to (2.6) this can be rewritten as

$$|\overline{v}|\ \le\ \delta \qquad (2.13)$$

(2.13) is of central importance in blunder detection. It shows that scaled residuals are "equally well checked" /15/ all over the network, and there-fore the maximal absolute scaled residual indicates the worse point with high probability. In ill conditioned systems and in systems with low relative redundancy symmetricities occur which result in high functional dependence among residuals. In such systems, especially with additional blunders present, such indication becomes uncertain or even singular /17/.

The geometric essence of the application of (2.13) remains as described by

---

[x] As treated in this section, blunder detection involves both the "detection" and the "location" of blunders, as defined by Stefanovic /17/.

(2.10) and (2.12)[x/] Therefore the sensitivity of blunder detection by this method is dependent on the geometric weight coefficient of the point in question. Considering (2.11) and (2.12) the tolerance can be based on some a-priori estimate σ^2 of the reference variance σ_o^2, and on some multiplyer to it defining bounds of "random" errors (as opposed to blunders) in the particular distribution, generally taken for 3. In such case the minimal undetectable blunder ∇_{min} can be written as

$$|\nabla_{min}| \leq 3\sigma(Q^+)^{-\frac{1}{2}} \qquad\qquad (2.14)$$

meaning, as compared with (2.10) and (2.11), that within these limits the blunder ∇ can be compensated by random influences. (2.14) shows another time that points of networks planned so to yield nearly equal (and dominating within Q_{vv}) geometric weight coefficients will be checked equally well.

2.2.2 Review of methods

First of all one should differentiate between methods of blunder detection aiming at individual differences as test values and those aiming at quadratic forms. Quadratic forms, especially when corresponding to large groups of points, are apt to hide small blunders. They are usually compared with tolerances determined with the help of the χ^2 or of the F-distribution. Stefanovic describes a better, partially empirical way of determining tolerances for quadratic forms which yields tighter values /17/. This improvement hardly can solve the problem for large groups of points, however.

x

As it has been shown in the previous section, the right way of checking

---

x/ This means that applying (2.13) for blunder detection corresponds to first, excluding temporarily the most suspicious point out of the adjustment as indicated by the maximal absolute scaled residual $|\bar{v}|$, and second, repeating the adjustment, and comparing $|v^-|$ of the temporarily excluded point with a tolerance depending upon geometric weight in accordance with (2.12). This direct way may be of advantage in computer programs especially when original error equations are not linear. So it is realized in program MODEL for checking relative orientation, as well.

individual differences is concerned with "scaled" residuals, as expressed
by (2.13). One can imagine two other ideas, in certain sense symmetric to
this way. The first has been intensively applied in the practice of least
squares, and aimes just at the individual residuals themselves.

$$|v_i| \lesssim \delta \qquad\qquad (2.15)$$

The second can be expressed as

$$|v_i^-| \lesssim \delta \qquad\qquad (2.16)$$

Taking into consideration the circumstance that a blunder distorts the en-
tire adjustment, blunder processing is in most cases concerned
the maximal in its absolute value difference. In the light of this (2.16)
corresponds to the checking of the maximal in its absolute value observa-
tional error (in the sense of (2.10)), determined by solving the equation
system n times, each time with n-1 observations involved, and always remov-
ing another point (!).

The exact way of setting tolerances in (2.15) has to proceed in correspond-
ence with (2.4), and for (2.16) in accordance with (2.12). In such way, as
far as tolerances are concerned, (2.15) and (2.16) go over in (2.13). When,
however, δ is set to a fixed value independent of the location of the point
(of the corresponding geometric weight coefficient), blunder detection with
(2.15) or (2.16) becomes less sensitive, especially in cases with low rela-
tive redundancy.

Apart from problems of sensitivity, the application of (2.15) and (2.16)
for finding the worse observation is theoretically inadequate, as shown
in connection with (2.13). The connected danger is rising with the relative
redundancy growing smaller.

<div align="center">x</div>

The theoretically most comprihensive strategy of blunder searching has
been described by Stefanovic /17/. Its essence is the following: one sup-
poses the presence of k blunders, taking k first for 1, and then, if nec-
essary, each time raising it by 1 and entering the process again. For k=1
the process corresponds to a checking according to (2.13). In addition,
the quadratic form corresponding to the rest of observations ($\bar{q}^2$) is com-

pared with a suitable tolerance. When k>1, groups of observations containing
k points each are checked and opposed to the rest of n-k points. All possible
combinations without repetition are checked. (2.6) in form of

$$\Delta = v_k^T \, (Q_{kk}^+)^{-1} v_k \qquad\qquad (2.17)$$

is applied. Both groups yield quadratic forms (Δ and $\bar{q}^2$) which are compared
with suitable tolerances. "All observations are blunders in those test groups
of the smallest size for which Δ exceeds the tolerance and $\bar{q}^2$ does not"/17/.

The weakness of this method lies in the lacking sensitivity of checking the
quadratic form $\bar{q}^2$. As a result, it works for k>1 only for large blunders.

<div align="center">x</div>

A more sensitive solution can be constructed by applying just (2.13), and
retaining the "error and trial" way of blunder processing which generally
has been applied for the last decades. This technique means always excluding
just the largest blunder, and repeating the adjustment with the rest of
data. Finally, all excluded observations are checked by the last solution,
and if needed, some of them taken back for a closing blunderfree adjustment.
What is very important: when adjusting linear models (not just linearized
ones), all the repeated adjustments may be constructed on the basis of a
single first adjustment with all the data included. For this, the needed
expressions are given in Stefanovic /17/.

The method proposed by Kraus /16/ is a special case which can be derived
from the theory given by Baarda /15/. Kraus's coefficient k_i equivalent
to $\bar{}_i$, and therefore his method is i   escr
previous paragraph.   aspects   by
work are: the formulas which connect adjustments with and without the blun-
ders (Stefanovic), the relationships proven in Appendices IX and X, and
a considerably better geometrical understanding of the processes (contri-
butions to the variance by groups of points by Stefanovic, the geometric
weight concept, and to some extent the interpretations grouped around for-
mulas (2.10) - (2.14) and (2.16)).

2.2.3 <u>Blunder detection as applied to analytical relative orientation</u>
      <u>and strip formation</u>

Table 2.1 provides a review of technologies of analytical aerial triangula-
tion as applied in our days. Processes are divided into three stages, re-
ferred to as first, second, and final. Data amount and applied degrees of
freedom grow drastically from one stage to the next. The same can be stated
about the costs of performing them.

Ideally, all stages had to contain processes of blunder detection. Technical
and economical considerations put limits to this. These limits are the more
prohibitive the more complex and the more expensive the process. In order
to provide guaranties against the widely spread phenomenon of (to put it
bluntly) "rough garbage in - smooth garbage out", sophisticated blunder de-
tection has to be applied at least in all preliminary stages.

The essential logic of basing blunder detection on the starting "differen-
tiated" stages is that of <u>sequential elimination</u>. So, the exclusion of points
with erroneous vertical parallaxes in the process of relative orientation
is inevitable for a successful blunder detection in model connection. Blunder
elimination in the process of model connection is of extreme importance for
strip homogenization. A "differentiated" (sequential) block adjustment,
whether polynomial or "of independent models", copes greatly safer with
blunders, when blunders in creating the models (or sections), and in pass-
points <u>within</u> each strip have been previously eliminated; and so on. In

<div align="right">

<u>Table 2.1</u>
</div>

Stages in computational technologies of analytical aerial triangulation

First	Second	Final
Relative orientation	Block adjustment	Simultaneous adjustment
(Strip formation)	- of independent models	of bundles of rays
	- of strip sections	
	- of triplets, quadrapelts,	
	etc.	
	Polynomial block adjustment	
	- of strips	
	- of strip sections	
	("piece-wise" polynomials)	

our opinion and experience, such sequential ways of blunder elimination are highly satisfactory and economical. In this respect we do not agree with Förstner /19/.

2.2.3.1 Numerical examples regarding aspects of blunder detection in analytical relative orientation

2.2.3.1.1 Point distribution; examples of Q_{vv}

Q_{vv} is a symmetric n x n matrix of rank r < n. Off-line elements in Q_{vv} express the functional dependence of residuals. The following expressions are valid /17/:

$$q_{ii} = \sum_{k=1}^{n} q_{ik}^2 \tag{2.18}$$

$$q_{ij} = \sum_{k=1}^{n} q_{ik}q_{jk} \tag{2.19}$$

$$0 \leq |q_{ij}| \leq q_{ii}q_{jj} \tag{2.20}$$

$$\sum_{i=1}^{n} q_{ii} = r \tag{2.21}$$

As a consequence of (2.21), the average diagonal element of Q_{vv} is equal to r/n.

A. Example with n = 6

In this case r = n - u = 1, and therefore all rows and columns of Q_{vv} are linear combinations of each other (they are proportional among themselves). This is an expression of the total uncertainty of blunder detection when r = 1: at the very best, the _presence_ of some blunder can be indicated but the blunder cannot be located.

N	Q_{vv}						Scheme of point distribution
1010	-.13	.06	-.09	.16	-.07		
1030	.25	-.13	.17	-.33	.14		
1050		.06	-.08	.16	-.07		
2010			.11	-.22	.10		
2030				.43	-.19		
2050	symmetric				.08		

Scheme of point distribution: 101, 103, 105

B. Example with n = 15

Scheme of point distribution   Scheme of distribution of $\sqrt{q_{ii}}$
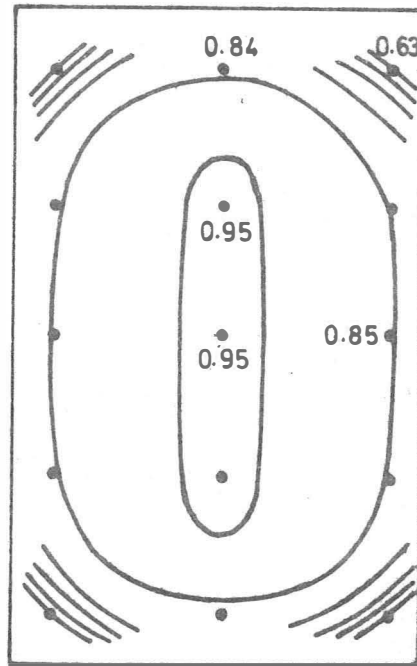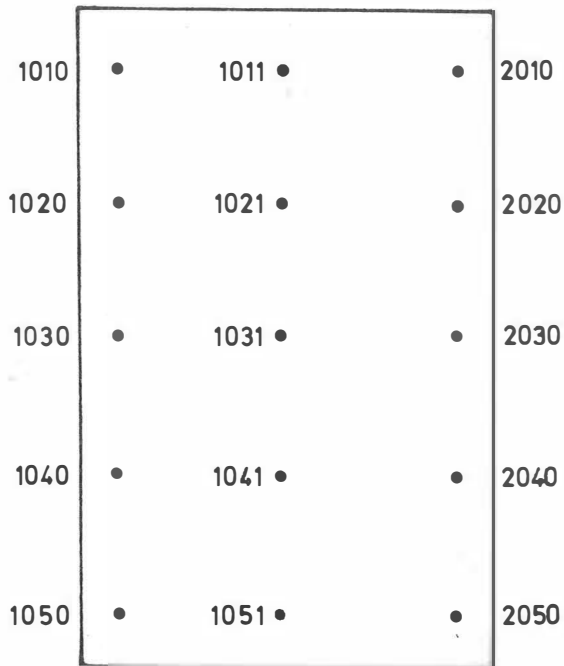
N	1010	1020	1030	1040	1050	1011	1021	1031	1041	1051	2010	2020	2030	2040	2050
1010	.38	-.27	-.05	.06	.05	-.30	-.09	.03	.04	-.04	.02	.09	.16	.05	-.13
1020		.69	-.24	-.12	.07	-.07	-.12	-.13	-.06	.06	.12	.03	-.04	-.01	.06
1030			.72	-.22	-.06	.03	-.10	-.16	-.10	.03	.11	.00	-.09	-.01	.13
1040				.73	-.28	.05	-.05	-.11	-.12	-.08	.04	.00	-.02	.03	.11
1050					.40	-.03	.03	.03	-.09	-.29	-.11	.03	.15	.11	.00
1011						.71	-.10	.02	.03	-.02	-.29	-.10	.04	.04	-.02
1021							.90	-.09	-.05	.03	-.11	-.10	-.10	-.05	.03
1031								.86	-.10	.02	.00	-.09	-.17	-.11	.02
1041									.89	-.09	.03	-.04	-.11	-.12	-.09
1051										.71	-.01	.02	.04	-.09	-.29
2010											.41	-.29	-.08	.04	.09
2020												.77	-.19	-.10	.02
2030													.69	-.22	-.06
2040														.73	-.29
2050	symmetric														.42

This example illustrates the important fact that an even point distribution does not result in an even distribution of geometric weights.

C. Example with n=10 evenly distributed points (minimal advicable set /11/)

Scheme of point distribution
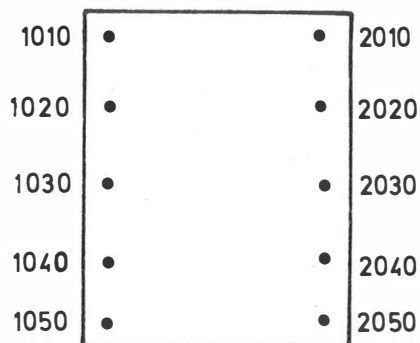
N	Q_{vv}									
1010		-.30	-.03	.08	.03	-.13	.04	.18	.07	-.15
1020		.63	-.29	-.14	.10	.07	-.02	-.10	-.04	.09
1030			.65	-.28	-.05	.12	-.03	-.16	-.06	.14
1040				.67	-.33	.05	-.02	-.07	-.03	.06
1050					.25	-.12	.03	.17	.06	-.13
2010						.27	-.36	-.08	.05	.10
2020							.72	-.23	-.12	.02
2030								.62	-.27	-.05
2040									.68	-.34
2050	symmetric									.28

D. Second example with n=10: less variance along the main diagonal, but with singular submatrix 1030 - 2030
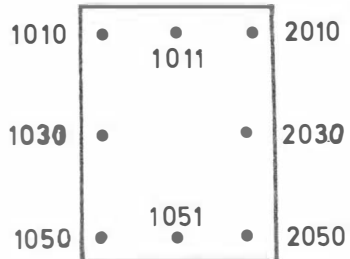
Scheme of point distribution
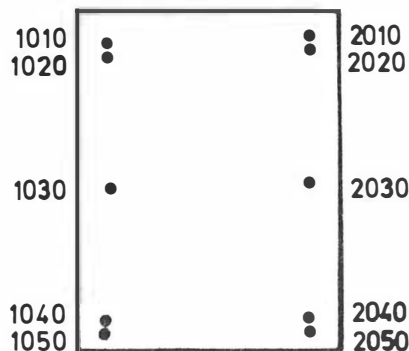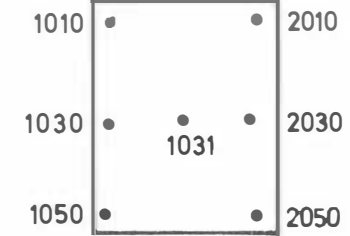
N	Q_{vv}									
1010	.52	-.48	-.09	.02	.02	-.02	-.02	.10	-.03	-.03
1020		.52	-.09	.02	.02	-.02	-.02	.10	-.03	-.03
1030			.38	-.10	-.10	.10	.10	-.40	.10	.10
1040				.52	-.48	-.02	-.02	.10	-.03	-.03
1050					.52	-.02	-.02	.10	-.03	-.03
2010						.52	-.48	-.10	.03	.03
2020							.52	-.10	.03	.03
2030								.42	-.11	-.10
2040									.53	-.47
2050	symmetric									.53
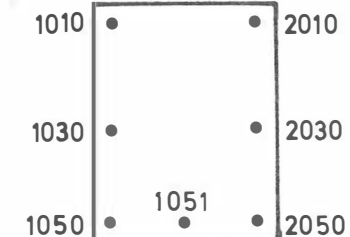
E. <u>Case with n = 8 (minimal acceptable set)</u>

N Q_{vv} Scheme of point distribution

N	1010	1030	1050	1011	1051	2010	2030	2050
1010	.24	-.16	.08	-.33	-.00	.08	.17	-.09
1030		.31	-.16	-.00	-.00	.16	-.33	.17
1050			.25	-.00	-.33	-.08	.17	.08
1011				.67	.00	-.33	-.01	.00
1051					.67	.00	-.01	-.33
2010						.25	-.17	.08
2030							.35	-.17
2050								.26

Scheme of point distribution:
1010 •   •   • 2010 (1011 at top center)
1030 •   • 2030
1050 •   •   • 2050 (1051 at bottom center)

F. <u>Two cases with n = 7 (both unacceptable for checking)</u>

N Q_{vv} Scheme of point distribution

N	1010	1030	1050	1031	2010	2030	2050
1010	.08	-.15	.08	-.01	-.08	.17	-.08
1030			-.16	-.31	.17	-.19	.18
1050			.08	-.01	-.08	.17	-.09
1031				.72	-.02	-.31	-.02
2010					.08	-.16	.09
2030						.49	-.17
2050	symmetric						.09

Scheme of point distribution:
1010 •   • 2010
1030 •   •   • 2030 (1031 at center)
1050 •   • 2050

N Q_{vv} Scheme of point distribution

N	1010	1030	1050	1051	2010	2030	2050
1010	.08	-.16	.08	.00	-.08	.16	-.08
1030		.31	-.15	-.00	.16	-.33	.17
1050			.08	-.33	-.09	.17	.08
1051				.67	.01	-.01	-.33
2010					.08	-.17	.08
2030						.35	-.17
2050	symmetric						.26

Scheme of point distribution:
1010 •   • 2010
1030 •   • 2030
1050 •   •   • 2050 (1051 at bottom center)

2.2.3.1.2 Error absorption

Tables 2.2 - 2.5 provide examples of error absorption in the process of
analytical relative orientation. In all cases, vertical parallaxes in all
points have been perturbed with random errors of $\sigma = \pm 0.01$ (mm), and in each
case one of the vertical parallaxes distorted with a blunder $\nabla = 0.05$ (mm).
When comparing "geometric weight coefficient matrices" Q_{vv} as given in
2.2.3.1.1, one can see that the last ones govern the extent of error ab-
sorption. The aim of tables 2.2 - 2.4 is to illustrate how the blunder
$\nabla = 5\sigma$ virtually disappears as a result of error absorption, and nevertheless

is rightly indicated by applying (2.13) - with the natural exception of
case 2.3 with r=1. Table 2.5 indicates that a point with a relatively
large "geometric weight coefficient" resists error absorption.

In all tables, σ_o is computed. An F-distribution test at significance lev-
el of 0.05 failes only in two of these cases. This indicates another time
that testing the reference variance σ_o is unsatisfactory for blunder de-
tection purposes /17/.

<div align="right">Table 2.2</div>

Point distribution: "E" in 2.2.3.1.1 or in table 2.6
Right side y of point 2010 distorted by 0.05 mm

	N	v	$\sqrt{q_{ii}}$	$\bar{v}$	
	1010	.004	.49	.009	
	1030	.004	.56	.007	
	1050	.001	.50	.001	
	1011	-.013	.82	-.016	
	1051	-.005	.82	-.006	
xxx	2010	.008	.50	.017	<-- max abs
	2030	-.004	.59	-.007	
	2050	.005	.51	.009	

$$\sigma_o = \pm .010$$
$$\sigma_o^2/\sigma^2 << F_{.05,3,\infty} \quad (1.0<<2.6)$$

<div align="right">Table 2.3</div>

Right side y of point 1010 distorted by 0.05 mm

	N	v	$\sqrt{q_{ii}}$	$\bar{v}$	
xxx	1010	.004	.28	.013	
	1030	-.007	.56	-.013	
	1050	.004	.28	.013	
	2010	-.004	.28	-.013	<-- max abs
	2030	.008	.56	.013	
	2050	-.004	.28	-.013	

$$\sigma \quad \pm .013$$
$$\sigma_o^2/\sigma^2 << F_{.05,1,\infty} \quad (1.7<<3.8)$$

Scheme of point distribution

Table 2.4

Point distribution: "B" in 2.2.3.1.1 or in table 2.6

Right side y of point 1010 distorted by 0.05 mm

N	v	$\sqrt{q_{ii}}$	$\bar{v}$	
xxx 1010	.027	.619	.043	<-- abs max
1020	-.022	.831	-.026	
1030	.002	.848	.003	
1040	.005	.849	.005	
1050	-.003	.631	-.005	
1011	-.025	.842	-.030	
1021	-.003	.948	-.004	
1031	.001	.924	.001	
1041	.014	.942	.015	
1051	-.002	.841	-.002	
2010	.003	.643	.005	
2020	.013	.876	.015	
2030	.003	.834	.003	
2040	-.006	.857	-.007	
2050	-.004	.647	-.006	

$$\sigma_o = \pm.015$$

$$\sigma_o^2/\sigma^2 > F_{.05,12,\infty} \quad (2.3 > 1.8)$$

Table 2.5

Point distribution: "E" in 2.2.3.1.1 or in table 2.6

Right side y of point 1051 distorted by 0.05 mm

N	v	$\sqrt{q_{ii}}$	$\bar{v}$	
1010	-.001	.494	-.002	
1030	-.006	.561	-.011	
1050	-.012	.498	-.025	
1011	.008	.816	.010	
xxx 1051	.031	.817	.038	<-- abs max
2010	-.007	.500	-.014	
2030	.006	.591	.010	
2050	-.019	.511	-.037	

$$\sigma_o = \pm.023$$

$$\sigma_o^2/\sigma^2 > F_{.05,3,\infty} \quad (5.3 > 2.6)$$

2.2.3.1.3 Comparative effectiveness of different ways of blunder detection

A series of numerical relative orientation examples has been computed with simulated data. Table 2.6 summarizes the results of 400 of them. There have been chosen 5 different characteristic point distributions (columns 1 and 6). Within each distribution, "rounds" of experiments have been computed, each round with a different value of a blunder (column 2). In table 2.6, each round is represented by one row. Within each round, n relative orientations have been performed (with n the number of points in the corresponding point distribution), and each time distorting the right side y" of another point by the corresponding blunder. Other points have been distorted by normally distributed δy" errors with a standard of ±0.01 mm. After the closing iteration, the points with max $|\bar{v}|$, max $|v^-|$, and with max $|v|$ have been found, and mistakes in indications of the blunder counted. Columns 3 - 5 of table 2.6 contain the results.

While the indicator max $|\bar{v}|$ shows no mistakes above a corresponding blunder level even in the case with n = 8 points (column 3), the indicators in columns 4 and 5 need 15 points for the same safety in blunder location.

Table 2.7 contains detailed results in one of the experiments participating in table 2.6 (n = 10, even distribution of points). Point 1010 in the corner of the model has been distorted. But because points in the corner possess very large "geometric weight", they influence the adjustment strongly, and past the adjustment show small residuals. In the case considered, the maximal $|v|$ occurs in point 1020. - Similar situations occur in all experiments within this point distribution pattern, when distorting one of the corner points.

Checking max $|v^-|$ causes still more troubles because residual dependence plays an important role in this case, as well.

No problems are accounted when checking max $|\bar{v}|$.

Table 2.8 contains detailed results for the experiment within point distribution "D", where the indicator max $|\bar{v}|$ failed in locating a blunder of 4σ (table 2.6). This is an example illustrating the danger of high dependence of two residuals. The corresponding submatrix of Q_{vv} is singular (2.2.3.1.1, "D"):

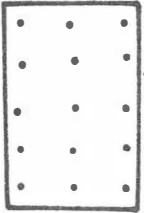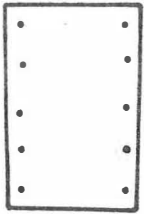$$D_{1030-2030} = \begin{vmatrix} 0.38 & -0.40 \\ -0.40 & 0.42 \end{vmatrix} \simeq 0$$

Table 2.6
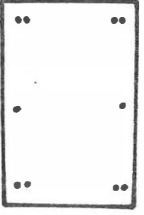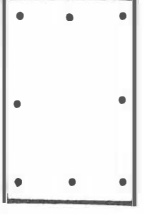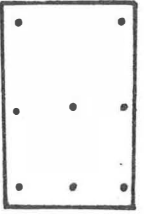
$\dfrac{n}{\sqrt{q_{ii}}_{\,min}}$	size of the blunder	Mistakes			Scheme of point distribution
		max $|\bar{v}|$	max $|v^-|$	max $|v|$	
1	2	3	4	5	6
$\dfrac{15}{====}$ 0.63	3 σ	2 13 %	4 27 %	3 20 %	"B"
	4 σ	0	2 13 %	2 13 %	
	5 σ	0	0	1 7 %	
	6 σ	0	0	1 7 %	
	7 σ	0	0	0	
	8 σ	0	0	0	
	9 σ	0	0	0	
	10 σ	0	0	0	
$\dfrac{10}{====}$ 0.50	3 σ	3 30 %	7 70 %	4 40 %	"C"
	4 σ	0	5 50 %	4 40 %	
	5 σ	0	5 50 %	4 40 %	
	6 σ	0	5 50 %	4 40 %	
	7 σ	0	5 50 %	4 40 %	
	8 σ	0	5 50 %	4 40 %	
	9 σ	0	5 50 %	4 40 %	
	10 σ	0	5 50 %	4 40 %	
$\dfrac{10}{====}$ 0.63	3 σ	2 20 %	1 10 %	2 20 %	"D"
	4 σ	1 10 %	1 10 %	1 10 %	
	5 σ	0	1 10 %	1 10 %	
	6 σ	0	1 10 %	1 10 %	
	7 σ	0	1 10 %	1 10 %	
	8 σ	0	1 10 %	1 10 %	
	9 σ	0	1 10 %	1 10 %	
	10 σ	0	1 10 %	1 10 %	
$\dfrac{8}{===}$ 0.50	3 σ	6 75 %	6 75 %	5 62 %	"E"
	4 σ	4 50 %	5 62 %	5 62 %	
	5 σ	2 25 %	4 50 %	5 62 %	
	6 σ	1 12 %	3 38 %	5 62 %	
	7 σ	1 12 %	3 38 %	5 62 %	
	8 σ	0	3 38 %	5 62 %	
	9 σ	0	3 38 %	5 62 %	
	10 σ	0	3 38 %	5 62 %	
$\dfrac{7}{===}$ 0.28	3 σ	3 43 %	6 86 %	5 71 %	"F"/1
	4 σ	3 43 %	6 86 %	5 71 %	
	5 σ	3 43 %	6 86 %	5 71 %	
	6 σ	2 28 %	6 86 %	5 71 %	
	7 σ	2 28 %	6 86 %	5 71 %	
	8 σ	2 28 %	6 86 %	5 71 %	
	9 σ	3 43 %	6 86 %	5 71 %	
	10 σ	3 43 %	6 86 %	5 71 %	

Table 2.7

Right side y of point 1010 distorted by 0.10 mm

	N	v	$\sqrt{q_{ii}}$	$\bar{v}$	
xxx	1010	.029	.481	.061	<-- abs max
	1020	-.041	.793	-.051	
	1030	-.000	.807	-.000	
	1040	.009	.816	.012	
	1050	.003	.504	.006	
	2010	-.016	.523	-.030	
	2020	.007	.850	.008	
	2030	.015	.784	.019	
	2040	.015	.825	.018	
	2050	-.021	.526	-.040	

Table 2.8

Right side y of point 2030 distorted by 0.040 mm

	N	v	$\sqrt{q_{ii}}$	$\bar{v}$	
	1010	.007	.723	.009	
	1020	.000	.723	.000	
	1030	-.014	.615	-.023	<-- abs max
	1040	.008	.725	.011	
	1050	-.002	.725	-.002	
	2010	-.010	.725	-.014	
	2020	.003	.725	.004	
xxx	2030	.014	.647	.022	
	2040	.005	.727	.007	
	2050	-.014	.727	-.019	

2.2.3.2.1 General processes of blunder detection in programs PHOTO and MODEL

Formal errors in recorded data, differences of repeated readings, and film deformation are checked in program PHOTO. This program contains a preliminary checking of data amount (for relative orientation and model connection), as well. All further checking is performed in program MODEL.

Blunder detection in relative orientation is performed in two connected processes: one of data amount and distribution checking, and second of applying (2.13) to (1.21). Each time, when a point has to be excluded, the first process is repeated before continuing the adjustment.

After the adjustment, vertical parallaxes in all "other" points (not having participated in the adjustment) are compared with a fixed tolerance inde-

pendent of the point's location.

Model connection is checked in a theoretically similar way. Beside pass-
point distribution and discrepancies in passpoints, parallelity of the
corresponding axes of model coordinate systems is checked. This last check-
ing results in warning messages.

(2.13) is not applied in strip homogenization as blunders have been exclud-
ed in the processes of sequential model connections. Discrepancies in pass-
points past strip homogenization are compared with tolerances independent
of the points' location. Rejected points do not appear in the output file
of strip coordinates.

Angular corrections determined in the process of strip homogenization are
compared with suitable tolerances, as well. This checking results in warn-
ing messages.

x

"Intermediate" and "final" tolerances are applied. Intermediate tolerances
are relevant to processes such as preliminary model connection by shifting
and scaling, while final tolerances apply to the final coordinates past
strip homogenization. Naturally, intermediate tolerances have to be some-
what looser.

Final tolerances in PHOTO and MODEL are a uniform system based upon a single
accuracy characteristic t of photogrammetric measurements (upon the standard
accuracy of measuring vertical parallaxes, as specified in input data). Some
options of the programs make interference with this system of tolerances
possible.

The whole system of tolerances is in the first line empirical, and evolved
in the process of some 12 years of application in widely varying circum-
stances. The following notes can be given on the most important elements
of this system:

   a/ in the practice, t is chosen between 0.010 and 0.015 mm-s; when work-
ing <u>exclusively</u> with signalized points, t can be chosen smaller;

   b/ deviations of repeated readings of image coordinates (or of readings
transverted to such coordinates) from their mean are kept within ± t;

c/ δ in (2.13) for relative orientation is taken for 3t;

d/ the "final" tolerance μ_{XY} for checking Y model coordinate discrepancies in passpoints is determined as follows:

In recent decades aerial photography for mapping purposes became highly standardized with regard to applying image format 23 x 23 cm^2, and a camera constant of 152 mm. This explaines the general belief according to which the accuracy of determining horizontal coordinates of terrain points, when ex-pressed in the scale of the photographs, yields a measure of photogrammetric performance suitable for comparisons. However this is not the case, it pro-vides good starting for most purposes.

Experience indicates that μ_{XY}, expressed in the scale of the photographs, is depending upon the image scale M (fig. 2.1). This has many reasons of quite different nature, nevertheless it has to be taken into account. There-fore the tolerance for checking Y model coordinate differences is determined in correspondence with μ_{XY} in fig. 2.1:

$$\mu_{XY} = 3t \ (1 + (M - 3000)/15000) \qquad \ldots (2.18)$$

where M is the denominator of the photo scale; if M < 3000, it is taken for 3000.

Fig. 2.1

e/ model coordinate discrepan-cies in Z are compared with a "fi-nal" tolerance μ_Z determined as

$$\mu_Z = 5 \ \frac{c}{p} \ t \qquad (2.19)$$

where p is some typical value of the horizontal parallax.

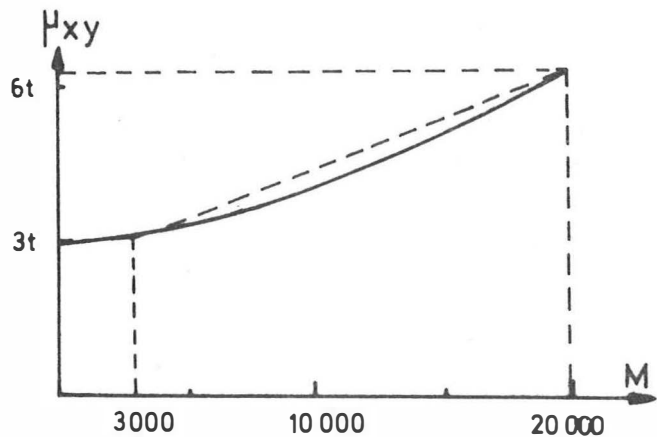In special cases, μ_{XY} and μ_Z have to be determined manually.

ACKNOWLEDGEMENTS

APPENDICES

CORRECTING IMAGE COORDINATES FOR SYSTEMATIC ERRORS

I.1 Film deformation

In case of side fiducials, a linear affine transformation takes care of
the task.

Corner fiducials control better the entity of the photograph, allowing a
more complex way of handling film deformation without the dangers of extra-
polation. The hyperbolic affine transformation described in /9/ has been
applied:

$$
\begin{bmatrix} a_{11} & a_{12} & a_{13} \\ a_{21} & a_{22} & a_{23} \end{bmatrix}
\begin{bmatrix} x_i - x_1 \\ y_i - y_1 \\ (X_i - X_1)(Y_i - Y_1) \end{bmatrix}
=
\begin{bmatrix} X_i - X_1 \\ Y_i - Y_1 \end{bmatrix}
\tag{I.1}
$$

where x_i, y_i denote the measured image coordinates,

X_i, Y_i the corrected image coordinates, and

$a_{11} - a_{23}$ the coefficients of the hyperbolic transformation.

It has to be emphasized that this transformation corresponds to a linear
interpolation of film deformation along straight lines (!).

Index 1 refers to the first fiducial. $a_{11} - a_{23}$ are determined by solving
two systems of linear equations with 3 unknowns, based upon (I.1) written
for fiducials 2-4 separately in x and y, and substituting calibrated (la-
boratory) coordinates for X_i and Y_i. All other points are transformed then
by (I.1) applied in two stages: first determining the approximate values
of corrected image coordinates X_i^o, Y_i^o by using just $a_{11} - a_{22}$, and then
counting the hyperbolic corrections (in program messages: the "torsion")
δX_t and δY_t as

$$
\delta X_{ti} = a_{13}(X_i^o - X_1)(Y_i^o - Y_1)
$$
$$
\delta Y_{ti} = a_{23}(X_i^o - X_1)(Y_i^o - Y_1)
\tag{I.2}
$$

Program PHOTO provides statistics of film deformation for each strip in
terms of "affine deformation" and the "torsion" mentioned before (see
Appendix II). Denoting by S the side length of a photograph, these deform-
ation characteristics are determined as

$$\text{affine deformation} = (\sqrt{\frac{a_{11}^2 + a_{12}^2}{a_{21}^2 + a_{22}^2}} - 1) \ S \qquad (I.3)$$

$$\text{torsion in } X = a_{13}S^2$$

$$\text{torsion in } Y = a_{23}S^2 \qquad (I.4)$$

For each strip, systematic, random standard, and maximal random statistics of the above deformation characteristics are determined. Both these statistics, and the individual values of deformation characteristics, are compared with suitable tolerances. Special attention is due to the values of systematic torsion in X and Y providing fine indication of the mechanical stability of the camera itself. Oscillations in individual torsion values indicate, generally, fiducial reading errors. Affine deformation is relatively susceptible to changes in circumstances and therefore less reliable for checking purposes.

(I.1) is applied in the process of joining readings of one and the same photographs in two positions in stereocomparators, as well ("left-to-right position transformations"). Statistics of these transformations provide an extremely reliable mean of checking fiducial readings of all intermediate photographs of a strip.

I.2 Optical distorsion

Only radial distorsion is handled. The corresponding formulas /13,14/:

$$\left.\begin{aligned}
r &= \sqrt{x^2 + y^2} \\
r_c &= r + \delta r \\
\delta r &= r(c_1 + c_3 r^2 + c_5 r^4 + c_7 r^6 + r(a \cdot \sin\alpha + b \cdot \cos\alpha)) \\
&= r(c_1 + c_3 r^2 + c_5 r^4 + c_7 r^6 + a \cdot y + b \cdot x)
\end{aligned}\right\} \qquad (I.5)$$

where x,y denote image coordinates, coefficients $a,b,c_1 - c_7$ describe optical distorsion, and index c stands for "corrected"; α is the direction angle of the vector pointing to the point.

I.3 Atmospheric refraction is corrected as described in /9/:

$$K = - \frac{2410\ H}{H^2-6H+250} - \frac{2410\ h}{h^2-6h+250} \frac{h}{H} \cdot 10^{-6}$$

$$r_c = K \left(1 + \frac{r^2}{c^2}\right)$$

$$\left. \right\} \quad (I.6)$$

where H denotes the flying height, and h the terrain height, both measured in kilometers above the sea level.

I.4 "Earth curvature" is no systematic error of image coordinates (as it often is treated) but a basic difference of the photogrammetric and of the geodetic coordinate systems. Therefore "Earth curvature" is not relevant to the processes of relative orientation and of strip formation.

APPENDIX II

Example of a REPORT file of programs PHOTO and MODEL

REPORT is an output file containing messages and statistics.

/see the next pages/

```
**********HOME WANO *** 78.11.07 *****************************************
```

```
                INITIAL DATA      FOCAL LENGTH =  152.67 MM
                                  FLYING HEIGHT    3500. M
                                  TERRAIN HEIGHT    600. M
                                  TOLERANCE         .015 MM
```

```
-----------------------------------------------------------------------
STRIP  1
```

```
                                          INPUT MODEL  61
                                          INPUT MODEL  62
                                          INPUT MODEL  63
```

STATISTICS OF LEFT-TO-RIGHT POSITION TRANSFORMATION

STANDARD FIDUCIAL READING ACCURACY   .0046 MM (REDUNDANCY= 24)

	SYSTEMATIC (MM)	STANDARD (MM)	MAXIMAL-RANDOM (MM)
TORSION IN X	.002	.007	.035 (PHOTO 63)
IN Y	.002	.017	-.012 (PHOTO 63)
AFFINE	-.006	.003	-.002 (PHOTO 62)

```
PHOTO  62 POINT        141
    OUT OF  4 (REDUCED) READINGS AT LEAST 1 ERRONEOUS:
                        115.375    65.518  <--
                        115.389    65.569
                        115.375    65.574
                        115.375    65.574

PHOTO  63 POINT        141
    OUT OF  6 (REDUCED) READINGS AT LEAST 2 ERRONEOUS:
                        36.922    76.855  <--
                        36.925    76.850
                        36.911    76.855
                        36.911    76.855
                        36.890    76.850  <--
                        36.902    76.859

PHOTO  63 POINT       6470
    OUT OF  4 (REDUCED) READINGS AT LEAST 1 ERRONEOUS:
                        118.004    91.004  <--
                        109.994    91.022
                        109.994    91.033
                        109.995    91.028
```

PHOTO BY PHOTO PROCESSING

```
        PHOTO  61

        PHOTO  62

        PHOTO  63

        PHOTO  64
```

STANDARD READING ACCURACY ON THE STRIP = .0064 MM (REDUNDANCY= 66)

STATISTICS OF FIDUCIAL TRANSFORMATION

	SYSTEMATIC (MM)	STANDARD (MM)	MAXIMAL-RANDOM (MM)
TORSION IN X	.005	.008	-.010 (PHOTO 64)
IN Y	-.026	.015	-.021 (PHOTO 64)
AFFINE	.010	.007	-.009 (PHOTO 64)

```
-----------------------------------------------------------------------
STRIP  2
```

```
                                          INPUT MODEL  27
                                          INPUT MODEL  28
                                          INPUT MODEL  29
```

STATISTICS OF LEFT-TO-RIGHT POSITION TRANSFORMATION

STANDARD FIDUCIAL READING ACCURACY   .0037 MM (REDUNDANCY= 6)

	SYSTEMATIC (MM)	STANDARD (MM)	MAXIMAL-RANDOM (MM)
TORSION IN X	.002	.014	.019 (PHOTO 29)
IN Y	-.003	.005	.003 (PHOTO 29)
AFFINE	-.007	.000	-.008 (PHOTO 29)

PHOTO BY PHOTO PROCESSING

```
        PHOTO  27

        PHOTO  28

        PHOTO  29

        PHOTO  30
```

STANDARD READING ACCURACY ON THE STRIP = .0056 MM (REDUNDANCY= 36)

*** FIDUCIAL READING ERROR, PHOTO 28 - TORSION IN X =   .046 MM ***

STATISTICS OF FIDUCIAL TRANSFORMATION

	SYSTEMATIC (MM)	STANDARD (MM)	MAXIMAL-RANDOM (MM)
TORSION IN X	-.013	.008	-.009 (PHOTO 30)
IN Y	.007	.019	.022 (PHOTO 27)
AFFINE	-.010	.015	-.015 (PHOTO 27)

```
                                  STRIP  2   *** FATAL ERROR ***
```

REPORT of program PHOTO

```
    TOLERANCES --

FOR REMAINDER Y-PAPALLAXES:   .045 MM
FOR MODEL CONNECTION DISCREPANCIES IN X AND Y:  1.416 MM (=  .0557 INCHES)
                                          IN Z:   .148 MM (=  .0058 INCHES)


    RELATIVE ORIENTATION  61 -  62

    RELATIVE ORIENTATION  62 -  63

    RELATIVE ORIENTATION  63 -  64



                        RESULTS AND STATISTICS


RELATIVE ORIENTATION
   PHOTO   PHI       OMEGA      KAPPA       RZ/BX    BY/PX  RMS OF D.PY
                  -- RADIANS, (GRADES) --                      MICRONS

   61  0.00000    0.00000    0.00000    .02352    .04900       9
       ( 0.000)   ( 0.000)   ( 0.000)   ( 1.497)  ( 3.117)
   62  .00699    -.00129    -.00066    .01100    .04418       4
       ( .445)    ( -.082)   ( -.042)   ( .700)   ( 2.810)
   63  .00151     .00899     .00511    .02752    .03631       7
       ( .096)    ( .572)    ( .326)    ( 1.751)  ( 2.310)
   64  -.00317    .00033     .00726
       ( -.202)   ( .021)    ( .462)



MODEL CONNECTION
   PHOTOS   RMS X   RMS Y   RMS Z    CORR. KAPPA        CORR. OMEGA
              -- MICRONS --         -- RADIANS, (DECIMAL SECONDS) --

   61 - 63     3      10      32    .00002 ( 12)      -.00043 ( -276)
   62 - 64     7      17      22
```

REPORT of program MODEL, t = 0.015 mm

```
    TOLERANCES --

FOR REMAINDER Y-PARALLAXES:   .030 MM
FOR MODEL CONNECTION DISCREPANCIES IN X AND Y:   .944 MM (=  .0372 INCHES)
                                          IN Z:   .098 MM (=  .0039 INCHES)


    RELATIVE ORIENTATION  61 -  62

    RELATIVE ORIENTATION  62 -  63

    RELATIVE ORIENTATION  63 -  64

PHOTOS 62- 64 MODEL CONNECTION: IMPROBABLE SYST. PART IN Z-DIFFERENCES
                    --- CHECK POINT TRANSFER ! ---



                        RESULTS AND STATISTICS

RELATIVE ORIENTATION
   PHOTO   PHI       OMEGA      KAPPA       RZ/BX    BY/PX  RMS OF D.PY
                  -- RADIANS, (GRADES) --                      MICRONS

   61  0.00000    0.00000    0.00000    .02352    .04900       9
       ( 0.000)   ( 0.000)   ( 0.000)   ( 1.437)  ( 3.117)
   62  .00699    -.00129    -.00066    .01100    .04418       4
       ( .445)    ( -.082)   ( -.042)   ( .700)   ( 2.810)
   63  .00151     .00899     .00511    .02752    .03631       7
       ( .096)    ( .572)    ( .326)    ( 1.751)  ( 2.310)
   64  -.00317    .00033     .00726
       ( -.202)   ( .021)    ( .462)



MODEL CONNECTION
   PHOTOS   RMS X   RMS Y   RMS Z    CORR. KAPPA        CORR. OMEGA
              -- MICRONS --         -- RADIANS, (DECIMAL SECONDS) --

   61 - 63     3      10      32    .00002 ( 12)      -.00043 ( -276)
   62 - 64     7      17      37
```

REPORT of program MODEL, repeated run, t = 0.010 mm

Abstract of a REPORT file as written by program MODEL. Data are simulated
so to illustrate effects of large errors in x. Messages for models 4 - 13
have been omitted here because they refraine those for the first models.
(Past the "fatal error" message the program runs further in a checking mode
of operation). The column of "RMS of d.py" (RMSE values of remainder verti-
cal parallaxes) indicates that the normally distributed errors of a standard
of ±0.1 mm, introduced into the x image coordinates, did not influence the
accuracy of the relative orientation (y image coordinates have been perturb-
ed with normally distributed errors of a standard of ±0.007 mm). However,
processes of model connection indicate these errors both in Y and Z. The
errors totally disappear in X model connection discrepancies (see Appendix
V).

/see the next page/

```
***********1  Y ERROR STANDARD 0.007, Y ERROF STANDARD 0.1 MM****************
STRIP  1


     TOLERANCES --

FOR REMAINDER Y-PARALLAXES:    .030 MM
FOR MODEL CONNECTION DISCREPANCIES IN X AND Y:   .050 MM (=  .0020 INCHES)
                               IN Z:   .102 MM (=  .0040 INCHES)


    RELATIVE ORIENTATION   1 -   2

    RELATIVE ORIENTATION   2 -   3

PHOTOS  1-  3 MODEL CONNECTION: IMPROBABLE SYST. PART IN Z-DIFFERENCES
                           --- CHECK POINT TRANSFER ' ---
PHOTOS  1-  3:         2010 FEROR IN TRANSFER
              (DX=  -.000, DY=    .589, DZ=   1.027), EXCLUDED
PHOTOS  1-  3:         2030 FEROR IN TRANSFER
              (DX=  -.000, DY=    .059, DZ=   1.436), EXCLUDED

 --- CHECK EVERY POINT ON PHOTO # 2 !!! ---
    RELATIVE ORIENTATION   3 -   4
PHOTOS  2-  4: NUMBER OF UNEXCLUDED PASSPOINTS
                        INSUFFICIENT FOR MODEL CONNECTION
MODEL CONNECTION   2-  4:
  DISCREPANCIES IN MM BEFORE THE CORRECTION PROCESS
    N      DX      DY      DZ
   3010    .000   -.005   -.167  <-- CHECK TRANSFER
   3020    .001   -.256  -1.293  <-- CHECK TRANSFER
   3030   -.000    .016    .219  <-- CHECK TRANSFER
   3040    .000   -.011   -.052
   3050    .001   -.623   1.158  <-- CHECK TRANSFER

 --- CHECK EVERY POINT ON PHOTO # 3 !!! ---


              *** STRIP    1: FATAL ERROR ***


    RELATIVE ORIENTATION   4 -   5
PHOTOS  3-  5: NUMBER OF UNEXCLUDED PASSPOINTS
                        INSUFFICIENT FOR MODEL CONNECTION
MODEL CONNECTION   3-  5:
  DISCREPANCIES IN MM BEFORE THE CORRECTION PROCESS
    N      DX      DY      DZ
   4010    .000   -.009    .049
   4020   -.000    .013    .134
   4030    .001   -.039   -.826  <-- CHECK TRANSFER
   4040    .000   -.004   -.184  <-- CHECK TRANSFER
   4050    .003    .627  -1.780  <-- CHECK TRANSFER

 --- CHECK EVERY POINT ON PHOTO # 4 !!! ---

              . . .
```

PESULTS AND STATISTICS

RELATIVE ORIENTATION					
PHOTO	PHI	OMEGA	KAPPA	BZ/BX	BY/BX	RMS OF D.PY
	-- RADIANS, (GRADES) --					MICRONS
1	0.00000	0.00000	0.00000	.05094	.00029	7
	(0.000)	(0.000)	(0.000)	(3.183)	(.018)	
2	.00242	.01367	-.00916	-.03071	.01037	12
	(.154)	(.870)	(-.583)	(-6.327)	(.004)	
3	.01125	-.00970	.00344	.05167	.00033	5
	(.716)	(-.618)	(.219)	(3.223)	(.021)	
4	.00484	-.01785	.00199	.00252	-.00208	9
	(.308)	(-.682)	(.126)	(.033)	(-.035)	
5	-.00451	.00826	-.00082	-.04032	.00014	9
	(-.287)	(.526)	(-.052)	(-7.137)	(.002)	
6	.01345	.01057	-.00210	.10043	.00067	9
	(.856)	(.673)	(-.134)	(6.372)	(.043)	
7	-.00269	-.01202	-.00146	-.04973	-.00008	13
	(-.172)	(-.765)	(-.729)	(-7.163)	(-.006)	
8	-.00846	.01475	.01130	.05017	.00349	7
	(-.539)	(.939)	(.723)	(3.191)	(.025)	
9	-.00675	-.00150	-.00976	-.09946	.00022	13
	(-.430)	(-.095)	(-.590)	(-6.311)	(.014)	
10	-.00355	-.01353	.00838	.05032	-.00027	6
	(-.226)	(-.861)	(.533)	(3.201)	(-.013)	
11	-.00344	-.00930	.00223	.05051	-.00041	6
	(-.219)	(-.592)	(.142)	(3.213)	(-.026)	
12	.00304	.00207	.00592	-.04935	-.00038	9
	(.193)	(.132)	(.377)	(-3.139)	(-.024)	
13	-.01349	.00695	-.01518			
	(-.668)	(.443)	(-.966)			

MODEL CONNECTION

PHOTOS	RMS X	RMS Y	RMS Z	CORR. KAPPA	CORR. OMEGA	
	-- MICRONS --			-- RADIANS, (DECIMAL SECONDS) --		
1 - 3	0	35	246	0.00000 (0)	0.00000 (0)	<-- CHECK
2 - 4	0	29	138	0.00000 (0)	0.00000 (0)	<-- CHECK
3 - 5	0	16	164	0.00000 (0)	0.00000 (0)	<-- CHECK
4 - 6	1	36	657	0.00000 (0)	0.00000 (0)	<-- CHECK
5 - 7	0	37	505	0.00000 (0)	0.00000 (0)	<-- CHECK
6 - 8	0	109	364	0.00000 (0)	0.00000 (0)	<-- CHECK
7 - 9	0	2	34	0.00000 (0)	0.00000 (0)	
8 - 10	0	29	112	0.00000 (0)	0.00000 (0)	<-- CHECK
9 - 11	1	217	473	0.00000 (0)	0.00000 (0)	<-- CHECK
10 - 12	0	82	183	0.00000 (0)	0.00000 (0)	<-- CHECK
11 - 13	1	582	972			<-- CHECK

No strip homogenization performed

SECOND SYSTEM OF FORMULAS

The expressions derived in chapter 1.2.2.2 can be transverted into functions of the right side photograph of the normal stereogram to be constructed. Considering $(S''S''_oM)$ in fig. 1 provides a key to this transversion:

$$
\begin{vmatrix}
0 & B_y & B_z \\
x''_t & y''_t & -c \\
x''_o & y''_o & -c
\end{vmatrix} = 0
$$

or

$$(x''_t y''_o - x''_o y''_t)\,\tan\tau + (x''_t - x''_o)\,\tan\nu = 0 \qquad\qquad (IV.15)$$

Adding (IV.15) to (1.5):

$$\frac{y''_t p_{xo} - x''_t p_{yo}}{c}\,\tan\tau + p_{xo}\tan\nu - p_y = 0 \qquad\qquad (IV.16)$$

where

$$p_{xo} = x' - x''_o$$

$$p_{yo} = y' - y''_o \simeq 0$$

$$p_y = y' - y''_t$$

(1.7),(1.9), and (1.14) after some elementary steps can be rewritten as

$$y''_o = y''_t + \frac{y''_t p_{xo} - x''_t p_{yo}}{c}\,\tan\tau + p_{xo}\tan\nu \qquad\qquad (IV.17)$$

$$\frac{y''_t p_{xo} - x''_t p_{yo}}{c}\,\tan\tau + p_{xo}\tan\nu - p_y = v \qquad\qquad (IV.18)$$

$$x''_o = x''_t\!\left(1 + \frac{p_{xo}}{c}\,\tan\tau\,\right) \qquad\qquad (IV.19)$$

where p_{xo} can be computed as

$$p_{xo} = \frac{x' - x''_t}{1 + \dfrac{x''_t}{c}\,\tan\tau} \qquad\qquad (IV.20)$$

(1.2) and (IV.18) yield the correction equation. The linearized form of it is:

$$(c+\frac{y_t''^2}{c})\delta\omega - \frac{x_t''y_t''}{c}\delta\phi + x_t''\delta\kappa + \frac{y_t''p_{xo} - x_t''p_{yo}}{c}\tan\tau + p_{xo}\tan\nu - (y'-y_t'') = v$$

$$\dots \text{(IV.21)}$$

The coefficients in (IV.21) contain x_t'', y_t'', p_{xo}, and p_{yo}, the precise value of which becomes known only in the last iterations ((IV.21) is a recursive expression).

For the x-direction - for purposes of further analysis - the following expression can be written, analogous to (IV.21):

$$- \frac{x''y''}{c}\omega + (c + \frac{x''^2}{c})\phi + y''\kappa + \frac{x''p_{xo}}{c}\tan\tau + R = \delta p_x \qquad \text{(IV.22)}$$

where R is the sum of non-linear terms in the expansion of (1.2), and

$$\delta p_x = p_{xo} - p_x = -\delta x'' = x'' - x_o''$$

X-discrepancies in passpoints

Differentiating the first row of (1.24) for the model S'S":

$$d(X')=d(\frac{B_x}{x_t'-x_o''} x_t')= \frac{B_x}{p_{xo}^2} (x_t'dx_o''-x_o''dx_t') \qquad \text{(V.1)}$$

Repeating the same for the model S"S"':

$$d(X'')=d(\frac{B_x}{x_t''-x_o'''} x_t'')= \frac{B_x}{p_{xo}^2} (x_t''dx_o'''- x_o'''dx_t'') \qquad \text{(V.2)}$$

The difference of (V.1) and (V.2) expresses the discrepancies in X model coordinates when substituting corresponding values for photo coordinates. Using the notation p for some typical value of the horizontal parallax, the following can be written for passpoints common to the above models:

$$x_t' \simeq p$$

$$x_o'' \simeq x_t'' \simeq 0 \qquad \text{(V.3)}$$

$$x_o''' \simeq -p$$

With these, (V.1) and (V.2) become equal to each other:

$$d(X') \simeq \frac{B_x}{P} \, dx_t'' \simeq d(X'')$$
(V.4)

meaning that their difference is equal to 0. For normal stereograms this can be seen geometrically in fig.1.2. The above deduction proves that this peculiarity remains in strength for a general case, as well. For grid points this is the exact truth. In practical cases this is a strong tendency (assumptions (V.3) are not exact in practical cases).

Appendix III contains a REPORT file of MODEL, illustrating the above described peculiarities.

It is quite interesting to note that discrepancies in x disappear not only in the process of relative orientation but in the process of model connection, as well. Such errors influence, however, the values of Y and Z via distorting the horizontal parallax. This can be seen in the second and third rows of (1.22), and very apparently, in Appendix III.

The conclusions of this appendix are meaningful for the theory of block adjustment of independent models. When (V.4) is valid, observation equations written for the block adjustment in X have to be given a high weight. In other words, (V.4) justifies a weighting in favour of strip continuity. (V.4) is valid when measurements of points belonging to one and the same photograph are checked and averaged before entering the process of relative orientation. This requirement is fulfilled in program PHOTO.

APPENDIX VI

Y-discrepancies in passpoints

Differentiating the second row of (1.24):

$$dY \simeq \frac{B_x}{P_{xo}} \left(\frac{1}{2}(dy_t'+dy_o'') - \frac{y}{P_{xo}} (dx_t'-dx_o'') \right)$$
(VI.1)

where

$$y = \frac{y_t' + y_o''}{2}$$

(1.2), (1.21), and (IV.22) yield expressions for dx_t', dy_t', dx_o'', and dy_o'':

$$dx'_t = \frac{x'y'}{c}d\omega' - (c + \frac{x'^2}{c})d\phi' - y'd\kappa'$$

$$dy'_t = (c + \frac{y'^2}{c})d\omega' - \frac{x'y'}{c}d\phi' + x'd\kappa'$$

$$dx''_o = \frac{x''y''}{c}d\omega'' - (c + \frac{x''^2}{c})d\phi'' - y''d\kappa'' - \frac{x''p_{xo}}{c}d\tau''$$

$$dy''_o = (c + \frac{y''^2}{c})d\omega'' - \frac{x''y''}{c}d\phi'' + x''d\kappa'' + \frac{p_{xo}y''}{c}d\tau'' + p_{xo}d\nu''$$

$$\left. \right\} \quad (VI.2)$$

For the triple overlap zone in fig. 1.2 we can assume:

$$x' \simeq p; \quad x'' \simeq 0; \quad x''' \simeq -p \qquad (VI.3)$$

where p corresponds to some typical value of the horizontal parallax. With (VI.3) one can wright expressions for the right side of model S'S" and for the left side of model S"S"'. The difference of these is the full ex-pression for discrepancies ΔY in passpoints. It contains, however, parts which become absorbed in connecting the models by (1.23). Excluding these constant and linear terms, we gain:

$$\Delta Y_a = -Y^2(\frac{1}{Z}\frac{d\omega''' - d\omega'}{2} + \frac{1}{B}(d\kappa''' - 2d\kappa'' + d\kappa')) \qquad (VI.4)$$

where the index "a" stands for "asymmetric". Taking into account that

$$d\omega''' - d\omega' = (d\omega''' - d\omega'') + (d\omega'' - d\omega') = \Delta\omega' + \Delta\omega''$$

and $\qquad\qquad\qquad\qquad\qquad\qquad\qquad\qquad\qquad\qquad\qquad\qquad (VI.5)$

$$d\kappa''' - 2d\kappa'' + d\kappa' = (d\kappa''' - d\kappa'') - (d\kappa'' - d\kappa') = \Delta\kappa'' - \Delta\kappa'$$

(VI.4) can be re-written in another form:

$$Y_a = -Y^2(\frac{1}{Z}\frac{\Delta\omega' + \Delta\omega''}{2} + \frac{1}{B}(\Delta\kappa'' - \Delta\kappa')) \qquad (VI.4')$$

APPENDIX VII

Z-discrepancies in passpoints

Differentiating the third row in (1.24):

$$dZ = \frac{B_x c}{p_{xo}^2}(dx'_t - dx''_o) \qquad (VII.1)$$

(VII.1) is an expression of the well known hyperbolic paraboloid. With

(VI.2) and (VI.3), and excluding constant and linear terms, an expression for ΔZ discrepancies in passpoints can be written:

$$\Delta Z = YZ(\frac{1}{Z} (d\omega'''-d\omega') + \frac{1}{B} (d\kappa'''-2d\kappa''+d\kappa')) \tag{VII.2}$$

Taking into account (VI.5):

$$\Delta Z = YZ(\frac{1}{Z} (\Delta\omega'+\Delta\omega'') + \frac{1}{B}(\Delta\kappa''-\Delta\kappa')) \tag{VII.2'}$$

<div align="right">APPENDIX VIII</div>

<u>Derivation of Q_{vv} for the case of indirect observations</u>

$$Ax = l + v = \breve{l} \tag{VIII.1}$$

$$v = \breve{l} - l = Ax - l$$

The solution of the corresponding normal equation system:

$$x = (A^T Q_{ll}^{-1} A)^{-1} A^T Q_{ll}^{-1} l$$

$$v = (A(A^T Q_{ll}^{-1} A)^{-1} A^T Q_{ll}^{-1} - I)l$$

$$Q_{vv} = (A(A^T Q_{ll}^{-1} A)^{-1} A^T Q_{ll}^{-1} - I)Q_{ll}(A(A^T Q_{ll}^{-1} A)^{-1} A^T Q_{ll}^{-1} - I)^T$$

$$= Q_{ll} - A Q_{xx} A^T \tag{VIII.2}$$

Taking into account (VIII.1):

$$Q_{\breve{l}\breve{l}} = A Q_{xx} A^T$$

$$\underline{Q_{vv} = Q_{ll} - Q_{\breve{l}\breve{l}}} \tag{VIII.3}$$

<div align="right">APPENDIX IX</div>

<u>Proving that $\sigma_o^2 = \frac{1}{n} \bar{v}^T \bar{W} \bar{v}$</u>

Notations: $\bar{Q} = \text{diag } Q_{vv}$

$$\bar{W} = \bar{Q}^{-1}$$

$$\overline{v}^T\overline{v} = v^T\overline{W}\,v$$

$$= (Ax-1)^T\overline{W}\,(Ax-1)$$

$$= x^TA^T\overline{W}Ax - 1^T\overline{W}Ax - x^TA^T\overline{W}1 + 1^T\overline{W}1$$

$$= x^TA^T\overline{W}Ax - 2x^TA^T\overline{W}1 + 1^T\overline{W}1$$

$$\text{as } x^TA^T = 1^T + v^T:$$

$$= x^TA^T\overline{W}Ax - 2(1^T + v^T)\overline{W}1 + 1^T\overline{W}1$$

$$= x^TA^T\overline{W}Ax - 1^T\overline{W}1 - 2v^T\overline{W}1$$

$$\text{as } v^T1 = v^T(Ax-v) = (x^TA^T - 1^T)Ax - v^Tv$$

$$= x^TA^TAx - 1^TAx - v^Tv = -v^Tv$$

$$(\text{as } A^TAx = Nx = A^T1)$$

$$v^T\overline{W}1 = -v^T\overline{W}v \qquad\qquad (IX.1)$$

$$= x^TA^T\overline{W}Ax - 1^T\overline{W}1 + 2v^T\overline{W}v \qquad\qquad (IX.2)$$

$$\overline{v}^T\overline{v} = v^T\overline{W}v = 1^T\overline{W}1 - x^TA^T\overline{W}Ax \qquad\qquad (IX.3)$$

$$\overline{W} = \sigma_o^2\,\overline{\Sigma}^{-1} \qquad\qquad (IX.4)$$

where $\overline{\Sigma}$ denotes the corresponding variance-covariance matrix taken for diagonal.

$$E\left[\overline{v}^T\overline{v}\right] = E\left[v^T\overline{W}v\right] = \sigma_o^2\,E\left[v^T\overline{\Sigma}^{-1}v\right] \qquad\qquad (IX.5)$$

On the basis of (IX.3), (IX.4), and (IX.5):

$$E\left[v^T\overline{\Sigma}^{-1}v\right] = E\left[1^T\overline{\Sigma}^{-1}1\right] - E\left[x^TA^T\overline{\Sigma}^{-1}Ax\right]$$

$$\text{as for symmetric } R \quad x^TRx = tr(xx^TR):$$

$$= E\left[tr(11^T\overline{\Sigma}^{-1})\right] - E\left[tr(Axx^TA^T\overline{\Sigma}^{-1})\right]$$

$$\text{with } \check{1} = 1 + v = Ax:$$

$$= tr(E\left[11^T\right]\overline{\Sigma}^{-1}) - tr(E\left[\check{1}\check{1}^T\right]\overline{\Sigma}^{-1})$$

$$\text{as } E\left[MM^T\right] = \Sigma_{MM} + \mu_M\mu_M^T:$$

$$= tr((\Sigma_{11} + \mu_1\mu_1^T)\overline{\Sigma}^{-1}) - tr((\Sigma_{\check{1}\check{1}} + \mu_{\check{1}}\mu_{\check{1}}^T)\overline{\Sigma}^{-1})$$

$$E\left[v^T\bar{\Sigma}^{-1}v\right] = tr((\Sigma_{11}-\Sigma_{\check{1}\check{1}})\bar{\Sigma}^{-1}) + tr((\mu_1\mu_1^T - \mu_{\check{1}}\mu_{\check{1}}^T)\bar{\Sigma}^{-1}) \qquad (IX.6)$$

$$Q_{vv} = Q_{11} - Q_{\check{1}\check{1}}$$

$$\Sigma_{vv} = \Sigma_{11} - \Sigma_{\check{1}\check{1}} \qquad (IX.7)$$

$$Ax = 1+v = \check{1}$$

$$\mu_{\check{1}} = \mu_{Ax} = E\left[Ax\right] = A\,E\left[x\right] = A\mu_x \qquad (IX.8)$$

$$1 = Ax - v$$

$$\mu_1 = E\left[1\right] = E\left[Ax\right] - E\left[v\right] = A\mu_x \qquad (IX.9)$$

(IX.6) with (IX.7), (IX.8), and (IX.6);

$$E\left[v^T\bar{\Sigma}^{-1}v\right] = tr((\Sigma_{11}-\Sigma_{\check{1}\check{1}})(\Sigma_{11}-\Sigma_{\check{1}\check{1}})^{-1}) +$$

$$tr((A\mu_x\mu_x^T A^T - A\mu_x\mu_x^T A^T)\bar{\Sigma}^{-1}) = tr(I) = n \qquad (IX.10)$$

(IX.5) with (IX.10):

$$E\left[\bar{v}^T\bar{v}\right] = n\sigma_o^2$$

which yields the expression sought:

$$\underline{\sigma_o^2 = \frac{1}{n}\,\bar{v}^T\bar{v}} \qquad (IX.11)$$

and, when $Q_{11} \neq I$:

$$\underline{\sigma_o^2 = \frac{1}{2}\bar{v}^T Q_{11}^{-1}\bar{v} = \frac{1}{n}\,v^T\bar{W}^{-\frac{1}{2}}\bar{W}\bar{W}^{-\frac{1}{2}}v} \qquad (IX.12)$$

APPENDIX X

Proving that $Q_{ff}^- = (Q^+)^{-1}$

where $Q_{ff}^- = I + A_i Q_{xx}^- A_i^T$

$$Q^+ = I - A_i Q_{xx}^+ A_i^T$$

Both Q_{ff} and Q^+ are counted for a group of k points, with $k \leq r$ (r - the re-

dundancy). A_i indicates the corresponding observation equations (k rows within A). Q_{ff} and Q^+ are k x k matrices.

$$Q_{xx}^+ = (A^T A)^{-1} \tag{X.1}$$

$$Q_{xx}^- = (A^T A - A_i^T A_i)^{-1} \tag{X.2}$$

The difference of inverses of (X.1) and (X.2):

$$(Q_{xx}^+)^{-1} - (Q_{xx}^-)^{-1} = A_i^T A_i$$

Multiplying from the left by $A_i Q_{xx}^-$, and from the right by $Q_{xx}^+ A_i^T$:

$$A_i Q_{xx}^- A_i^T - A_i Q_{xx}^+ A_i^T = (A_i Q_{xx}^- A_i^T)(A_i Q_{xx}^+ A_i^T)$$

Adding the unit matrix to both sides, and rearranging:

$$I = I + A_i Q_{xx}^- A_i^T - A_i Q_{xx}^+ A_i^T - (A_i Q_{xx}^- A_i^T)(A_i Q_{xx}^+ A_i^T)$$

$$I = (I + A_i Q_{xx}^- A_i^T)(I - A_i Q_{xx}^+ A_i^T)$$

Multiplying by $(I - A_i Q_{xx}^+ A_i^T)^{-1}$ yields the sought expression (this inverse generally exists because k<r):

$$I + A_i Q_{xx}^- A_i^T = (I - A_i Q_{xx}^+ A_i^T)^{-1} \tag{X.3}$$

or

$$\underline{Q_{ff}^- = (Q^+)^{-1}} \tag{X.4}$$

References

1. Shut, G.H.: An Introduction to Analytical Strip Triangulation with a
        FORTRAN Program. NRC-9396, 1966

2. Skiridow, A.S.: Stereophotogrammetry (in Russian). Moscow, Geodezizdat,
        1957

3. Jerie, H.G.: Beitrag zu numerischen Orientierungsverfahren für gebirgi-
        ges Gelände. Photogrammetria, X., 1953-54, No.1

4. Pope, A.J.: Some Pitfalls to be Avoided in the Iterative Adjustment of
        Nonlinear Problems. American Society of Photogrammetry,
        Proceedings of the 38-th Annual Meeting, March, 1972

5. Lobanow, A.: Phototriangulation applying computers (in Russian).
        Moscow, Geodezizdat, 1960 and Moscow, Njedra, 1967

6. Schwidefsky, K. und Ackermann, F.: Photogrammetrie. Stuttgart,
        B.G.Teubner, 1976

7. Lehman, G.: Die Verwendung von Bildpaaren und Bildtripeln bei der Aero-
        triangulation von Bildstreifen. Z.f.Vermessungswesen, 1963

8. Mikhail, E.M.: Use of Triplets for Analytical Aerotriangulation.
        Photogrammetric Engineering, 1962

9. Harris, W.D., Tewinkel, S.C., and Whitten, C.A.: Analytic Aerotriangu-
        lation. Coast and Geodetic Survey, Technical Bulletin No.21,
        July 1962, corrected July 1963

10. Urmayev: Elements of Photogrammetry (in Russian). Moscow, Geodezizdat,
        1941

11. Waldhäusl, P.: Beitrag zur Untersuchung systematischer Fehler der Aero-
        triangulation. Dissertation, TU Wien, 1968

12. Molnar, L.K.: Self Checking Analytical Strip Formation by Programs
        PLATE and MODEL. Program documentation, Berger Associates,
        Columbus, Ohio, 1976

13. Kraus, K., Stark, E.: Flächenhafte Verzeichnungskorrektur in der nume-
        rischen Photogrammetrie. Bildmessung und Luftbildwesen,
        2/1973, S.50-56

14. Vlcek, J.: Systematic errors of image coordinates. Photogrammetric
        Engineering, 1969, pp.585-593

15. Baarda, W.: A Testing Procedure for Use in Geodetic Networks. Nether-
        lands Geodetic Comission, Publications on Geodesy, New
        Series, Vol.2, No.5, 1968

16. Kraus, K.; Verschiedene Transformationen und Indikatoren zur Lokali-
        sierung grober Datenfehler. Allgemeine Vermessungs-Nachrich-
        ten, Heft 1/1975
17. Stefanovic, P.: Blunders and Least Squares. The ITC Journal, 1978-1
18. Mikhail, E.M.: Observations and Least Squares. IEP-A Dun-Donnelley
        Publisher, New York, 1976
19. Förstner, W.: Die Suche grober Fehler in Photogrammetrischen Lageblöcken.
        Dissertation, Stuttgart, 1977
20. Marks, G.W., Mikhail, E.M., McGlone, J.C.: Comparative Analysis of
        Block Triangulation by Bundles and Stereo-Units. Technical
        Report, School of Civil Engineering, Purdue University,
        West Lafayette, Indiana 47907, July, 1978

Bisher erschienen:

Heft 1 Kolloquium der Assistenten der Studienrichtung Vermessungs-
wesen 197o - 1973, Dezember 1973.

Heft 2 EGGER-PERDICH-PLACH-WAGENSOMMERER, Taschenrechner HP 45
und HP 65, Programme und Anwendung im Vermessungswesen,
1. Auflage, März 1974, Special Edition in English, Juli 1974,
2. verbesserte Auflage, November 1974.

Heft 3 Kolloquium der Assistenten der Studienrichtung Vermessungs-
wesen 1973 - 1974, September 1974.

Heft 4 EGGER-PALFINGER-PERDICH-PLACH-WAGENSOMMERER, Tektronix-
Tischrechner TEK 31, Programmbibliothek für den Einsatz
im Vermessungswesen, November 1974.

Heft 5 K. LEDERSTEGER, Die horizontale Isostasie und das iso-
statische Geoid, Februar 1975.

Heft 6 F. REICHHART, Katalog von FK4 Horrebow-Paaren für Breiten
von + 30° bis + 60°, Oktober 1975.

Heft 7 Arbeiten aus dem Institut für Höhere Geodäsie, Wien,
Dezember 1975.

Heft 8 Veröffentlichungen des Instituts für Photogrammetrie zum
XIII. Internationalen Kongreß für Photogrammetrie in
Helsinki 1976, Wien, Juli 1976.

Heft 9 Veröffentlichung des Instituts für Kartographie und
Reproduktionstechnik, W.PILLEWIZER, Felsdarstellung aus
Orthophotos, Wien, Juni 1976.

Heft 10 PERDICH-PLACH-WAGENSOMMERER, Der Einsatz des programmier-
baren Taschenrechners Texas Instruments SR-52 mit Drucker
PC-100 in der ingenieurgeodätischen Rechentechnik, Wien,
Mai 1976.

Heft 11 Kolloquium der Assistenten der Studienrichtung Vermessungs-
wesen 1974 - 1976, November 1976.

Heft 12 Kartographische Vorträge der Geodätischen Informations-
tage 1976, Wien, Mai 1977.

Heft 13 Veröffentlichung des Instituts für Photogrammetrie anläßlich
des 80. Geburtstages von Prof. Dr.h.c. K. Neumaier,
Wien, Januar 1978.